Extrasolar Planets

Introduction

So far: have looked at planets around our Sun

Physics question:

Is our Solar System normal?

⟹ Are there planets around other stars?

can then compare solar system with other systems.

To answer these questions, we need to detect extrasolar planets.

Detection Methods

Possible ways to detect extrasolar planets:

Direct Method:

- . . . direct imaging of planet (visual binary)

Indirect Methods: search for evidence for. . .

- . . . radial velocity: Motion of host star (spectroscopic binary)
- . . . periodic variation of proper motion of the star (like Sirius) astrometric binary
- photometry: light curves: occultation (transits)
- others (not discussed here):
  - . . . influence of planet on light from behind planet (gravitational lensing)
  - . . . time of flight variations (pulsars, pulsating stars)

Direct Imaging

In order to make an image of an extrasolar planet, need to separate images of star and planet with telescope

⟹ Requires two ingredients:

1. “contrast” (relative intensity of star and planet)
2. “resolving power” of telescope (angular distance between star and planet)

Direct Imaging: Contrast

Estimate intensity contrast between star and planet:

Solar system: Luminosity of Sun $L = 3.90 \times 10^{26}\,\mathrm{W} =: L_\odot$

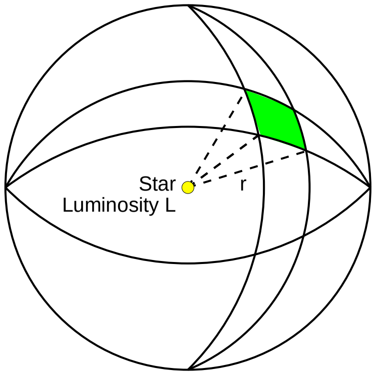

This power is emitted isotropically into all directions.

Direct Imaging: Contrast

Estimate intensity contrast between star and planet:

Solar system: Luminosity of Sun $L = 3.90 \times 10^{26}\,\mathrm{W} =: L_\odot$

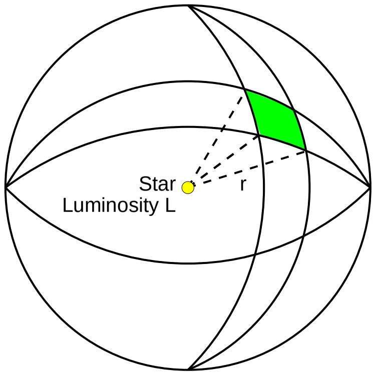

This power is emitted isotropically into all directions.

$\Longrightarrow$ Energy received per second on whole area of sphere of radius r (area $A = 4\pi r^2$) equals L as well!

Direct Imaging: Contrast

Estimate intensity contrast between star and planet:

Solar system: Luminosity of Sun $L = 3.90 \times 10^{26}\,\mathrm{W} =: L_\odot$

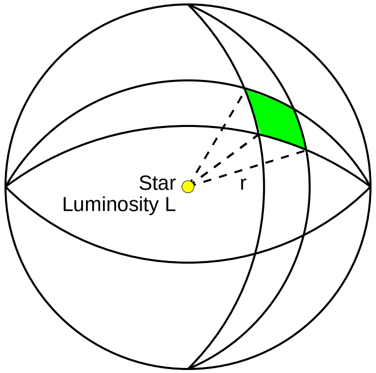

This power is emitted isotropically into all directions.

$\Longrightarrow$ Energy received per second on whole area of sphere of radius r (area $A = 4\pi r^2$) equals L as well!

$\Longrightarrow$ Energy falling per second on area of $1\,\mathrm{m}^2$ at distance r (“flux”):

$$F = \frac{L}{4\pi r^2}$$

units: $\mathrm{W\,m^{-2}}$ or $\mathrm{erg\,cm^{-2}\,s^{-1}}$

Direct Imaging: Contrast

Plugging in typical numbers:

Earth:

distance: $r = 1\,\mathrm{AU} = 150 \times 10^6\,\mathrm{km}$

$\Longrightarrow P \sim 1380\,\mathrm{W\,m^{-2}}$ (“solar constant”).

Total power received by Earth: projected solar facing area $A = \pi r_\oplus^2 = 1.26 \times 10^{14}\,\mathrm{m}^2$

$\Longrightarrow$ Total power received: $P_{\text{total},\oplus} = 1.74 \times 10^{17}\,\mathrm{W}$.

Of this, about 30% is reflected, i.e., $L_\oplus = 5.2 \times 10^{16}\,\mathrm{W} \sim 10^{-10}\,L_\odot$.

The luminosity of the Earth is 10 billion times weaker than that of the Sun.

in infrared, luminosity contrast is only 10 million, but still rather weak. . .

Direct Imaging: Contrast

Plugging in typical numbers:

Jupiter:

distance: $r = 5.2\,\text{AU} = 7.8 \times 10^8\,\text{km} \Longrightarrow P \sim 51\,\text{W}\,\text{m}^{-2}$

Total power received by Jupiter: projected solar facing area $A = \pi r_{♃}^2 = 1.6 \times 10^{16}\,\text{m}^2$

$\Longrightarrow$ Total power received: $P_{\text{total},♃} = 8.2 \times 10^{17}\,\text{W}$.

Of this, about 30% is reflected, i.e., $L_{♃} = 2.5 \times 10^{17}\,\text{W} \sim 6 \times 10^{-10}\,L_\odot$.

The luminosity of Jupiter is ~1 billion times weaker than that of the Sun.

$\Longrightarrow$ For typical planets around solar type stars, we need to be able to detect intensity contrasts of better than 1:1 billion.

$\Longrightarrow$ Not doable now, but not unrealistic to achieve in your lifetime (“coronagraphs”)...

Direct Imaging: Angular Separation

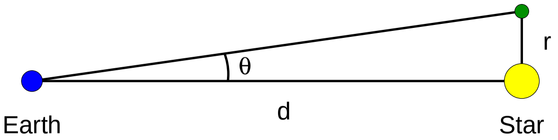

How close on sky are images of Sun and planet?

$$\tan\theta = \frac{r}{d} \quad\Longrightarrow\quad \theta \sim \frac{r}{d}$$

(for small θ: Taylor series: $\tan\theta \sim \theta + (1/3)\theta^3 + \ldots$; “small angle approximation”)

Typical distances to nearby stars: $d \sim 100\,\text{Ly} = 9.5 \times 10^{17}\,\text{m}$,

typical distances in planetary system: $r \sim 1\,\text{AU} = 1.5 \times 10^{11}\,\text{m}$,

$$\Longrightarrow \qquad \theta = \frac{r}{d} = 1.57 \times 10^{-7}\,\text{rad} = 9 \times 10^{-6}\,\text{deg} = 0.03''$$

reminder: $1'' = 1\,\text{arcsec} = 1/3600\,\text{deg}$.

Direct Imaging: Angular Separation

Optics: resolving power of telescope with diameter D:

$$\alpha = \frac{12''}{D/1\,\text{cm}} \tag{9.8}$$

$\Longrightarrow$ to resolve $0.03''$, need $D = 4\,\text{m}$, so doable

BUT

Earth atmosphere limits resolution to $\sim 0.5''$ (“seeing”)

Currently, direct detection of extrasolar planets around solar-type stars is not doable from ground, although it is technologically feasible from space.

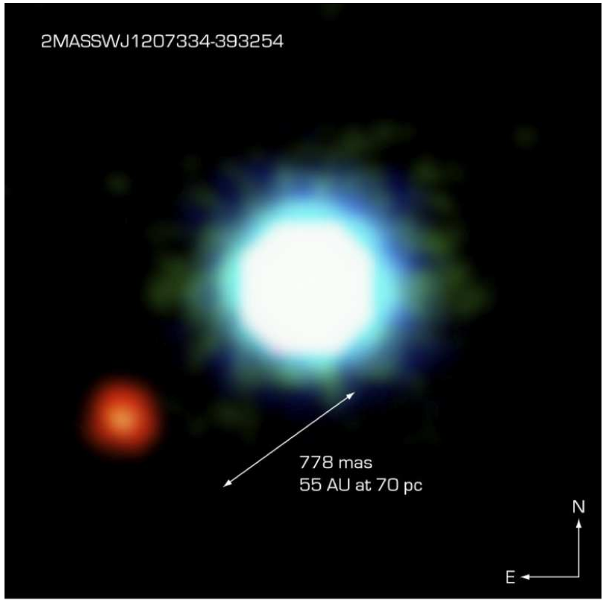

The Brown Dwarf 2M1207 and its Planetary Companion (VLT/NACO)

ESO PR Photo 14a/05 (30 April 2005)

Using adaptive optics, it is possible to obtain diffraction limited resolution in the near infrared.

Contrast is still a problem, however, for one very dim star (a “brown dwarfs”) a planetary companion was detected in early 2005 with the VLT and confirmed in 2006 with HST.

Distance between star and planet: ~2× Neptune distance, distance to system $59 \pm 7\,\text{pc}$.

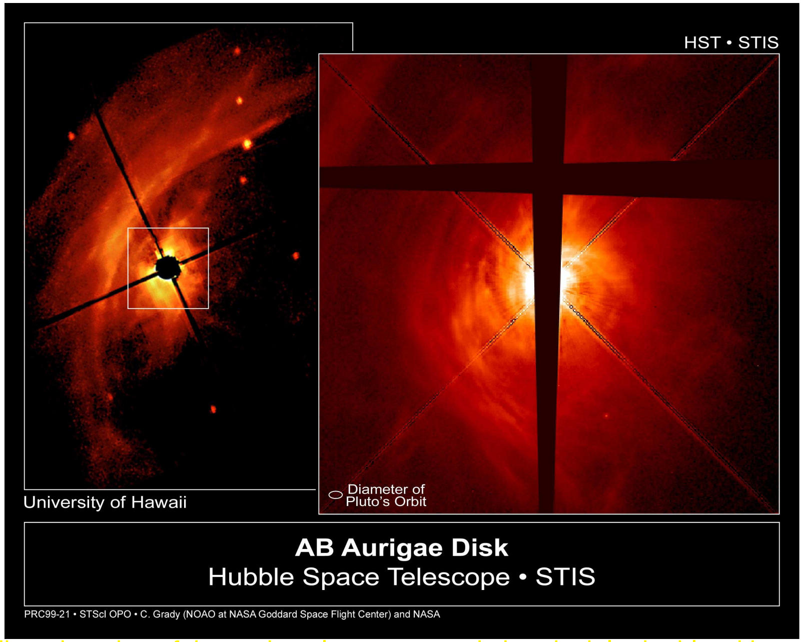

. . . direct imaging of the region close to a star is in principle doable with modern technology (HST, VLT, et al.)

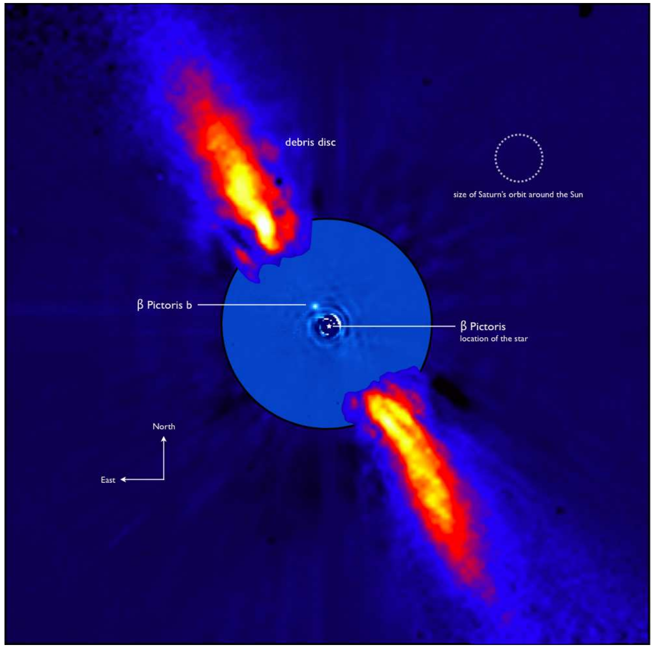

ESO

21.11.2008: Direct imaging of planet with ESO-VLT and NACOS instrument announced (planet around β Pictoris, 1000× fainter than star).

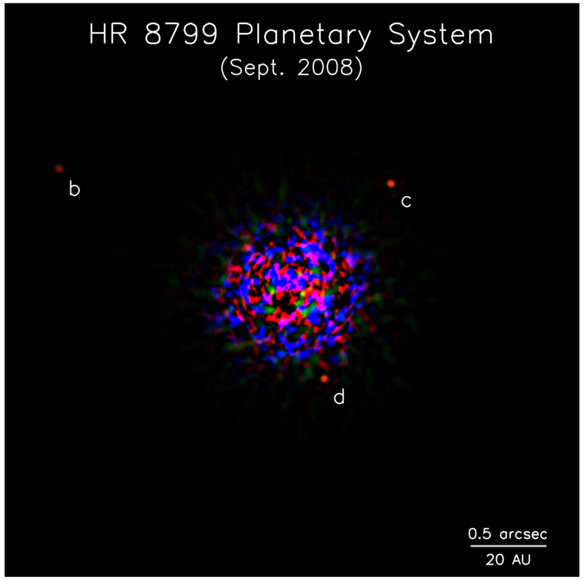

C. Marois (NRC-HIA), IDPS survey and Keck Observatory

13.11.2008: Direct imaging of planetary system around HR 8799 announced; distances 70, 40, and 25 AU from star (constellation Pegasus; $d = 110$ Ly).

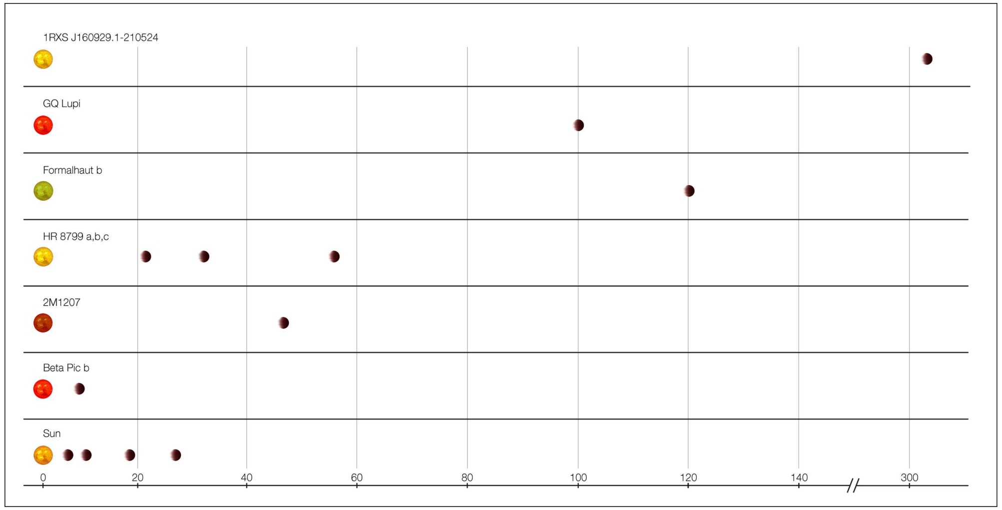

ESO

Overview of all systems with imaged planets

Radial Velocity Measurements

If we cannot see planet directly $\Longrightarrow$ use indirect methods.

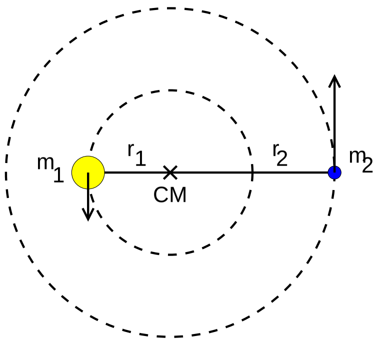

Two-body problem: Star and planet move around common center of mass:

$$m_1 r_1 = m_2 r_2$$

For circular orbits and orbital period P, velocity of star due to action of planet is

$$v_1 = \frac{2\pi r_1}{P} = \frac{2\pi}{P} \cdot \frac{m_2}{m_1} \cdot r_2$$

Example: Sun vs. Jupiter:

$m_1 = 2 \times 10^{30}\,\mathrm{kg}$, $m_2 = 2 \times 10^{27}\,\mathrm{kg}$, $r_2 = 5.2\,\mathrm{AU} = 7.8 \times 10^{11}\,\mathrm{m}$, $P_\mathrm{J} = 11.9\,\mathrm{yr} = 3.76 \times 10^{8}\,\mathrm{s}$

$\Longrightarrow v_1 = 13.1\,\mathrm{m\,s^{-1}} \sim 50\,\mathrm{km\,h^{-1}}$

Example: Sun vs. Earth gives $v_1 = 10\,\mathrm{cm\,s^{-1}} \sim 0.8\,\mathrm{km\,h^{-1}}$

Radial Velocity Measurements

Doppler motion of the sun due to all planets in the solar system as an observer in the ecliptic would have measured:

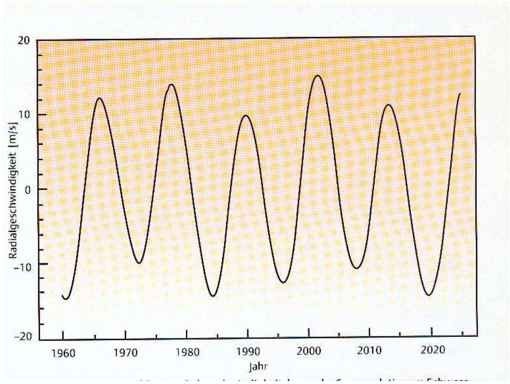

- Superposition of sinusoidal radial velocity curves.
- amplitude = $13\,\mathrm{m\,s^{-1}}$
- Largest effect due to Jupiter.

need to measure stellar radial velocity to much better than $13\,\mathrm{m\,s^{-1}}$.

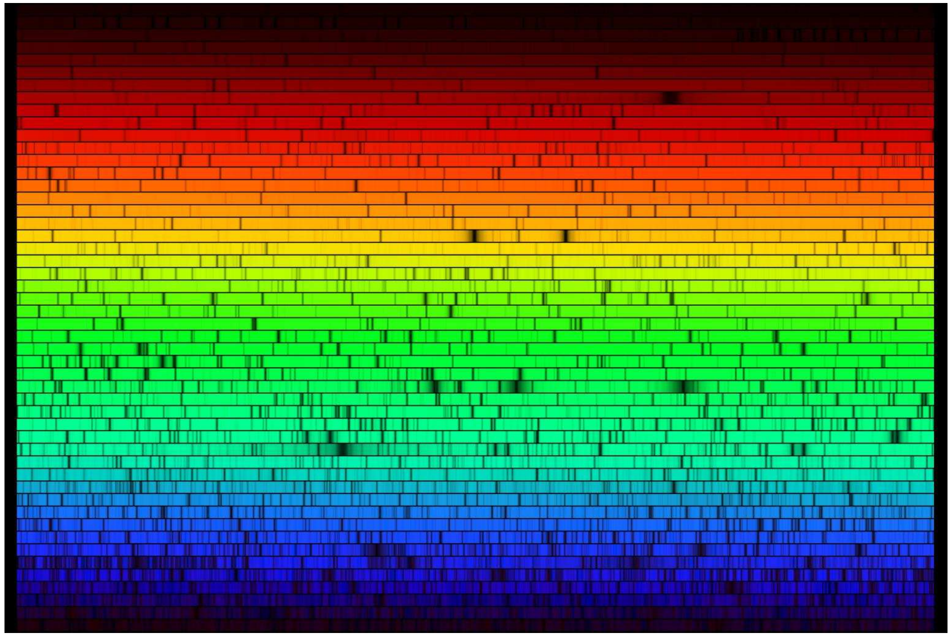

N.A. Sharp, NOAO/NSO/Kitt Peak FTS/AURA/NSF

Absorption line spectrum of the Sun: Fraunhofer Lines

Radial Velocity Measurements

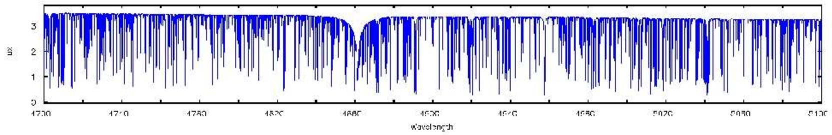

Doppler motion of the sun:

$$\frac{\lambda_\text{observed} - \lambda_\text{emitted}}{\lambda_\text{emitted}} = \frac{v}{c} \quad \text{with } v = 13\,\mathrm{m\,s^{-1}}\text{:} \quad \Delta\lambda/\lambda = 4 \times 10^{-8} \tag{11.1}$$

Line broadening due to thermal motion of the light emitting ions:

$$v^2_\text{therm} = \frac{2kT}{Am_\mathrm{H}} \Longrightarrow \frac{\Delta\lambda}{\lambda} = \frac{2kT}{Am_\mathrm{H}c} \tag{11.2}$$

where A: atomic weight in atomic mass units (m_H)

For the Sun ($T = 5780\,\mathrm{K}$):

- Hydrogen: $v_\text{therm}(\mathrm{H}) = 9.8\,\mathrm{km\,s^{-1}} \Longrightarrow \frac{\Delta\lambda}{\lambda} = 3 \times 10^{-5}$
- Iron: $v_\text{therm}(\mathrm{Fe}) = 1.3\,\mathrm{km\,s^{-1}} \Longrightarrow \frac{\Delta\lambda}{\lambda} = 4 \times 10^{-6}$ (prefer heavy elements!)

Intrinsic line widths are 400–3000 times larger than expected Doppler velocity.

Radial Velocity Measurements

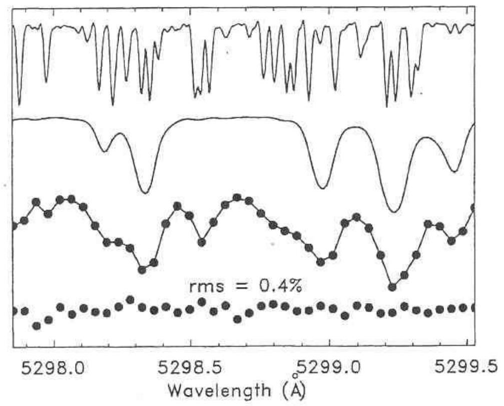

- accuracy can only be reached by measuring tens of thousands of lines
- long term stability: very stable wavelength standard needed
- Iodine cell in front of spectrograph: Iodine vapor at ∼50° C. High mass (127), low temperature $\Longrightarrow$ sharp lines.
- cross correlation of spectra.
- works with cool stars, e.g., solar-like (sufficient number of lines).

Radial Velocity Measurements

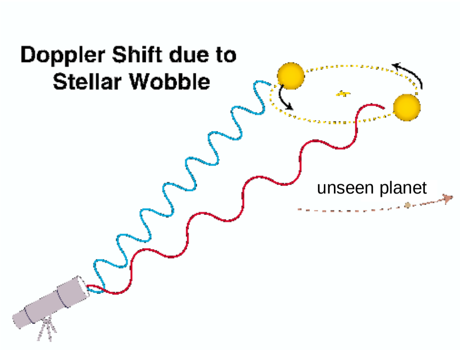

G. Marcy

How to hunt extrasolar planets using the Doppler Detection Method:

1. get access to *lots* of telescope time
2. get access to *very good* spectrograph
3. measure for years, to determine changes in velocity of stars due to motion of star around CM

Astrometry

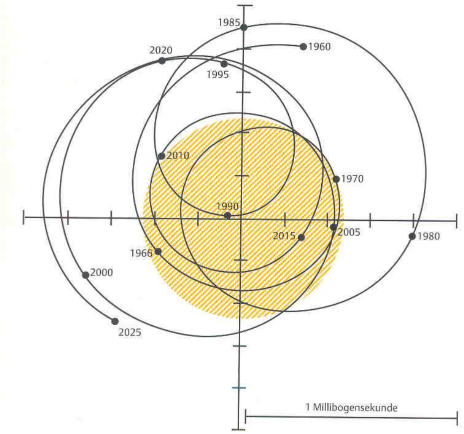

Motion of the sun around the center of gravity viewed from above from 10 pc distance

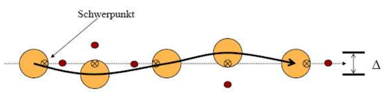

Outlook:

- planet+star: astrometric binary
- measure periodic wobble of the proper motion
- need precision <1 mas, not achieved yet
- GAIA astrometric mission of ESA to be lauched in 2011

Transits

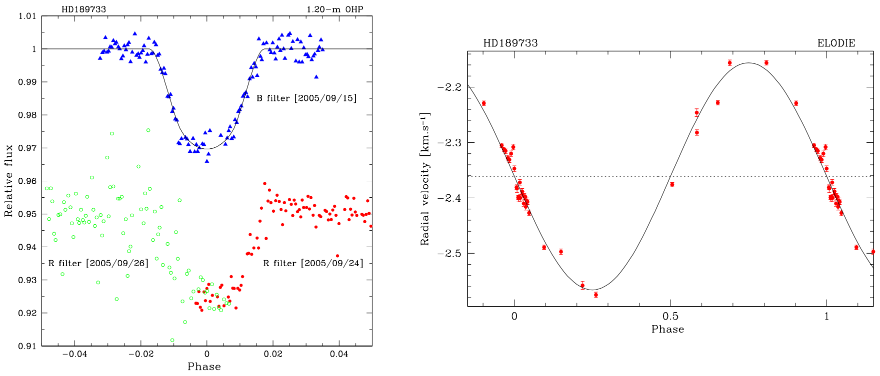

Planetary transit: occultation of the star by the planet

$\Longrightarrow$ inclination known

Can determine mass *and* radius of the planet!

Transits

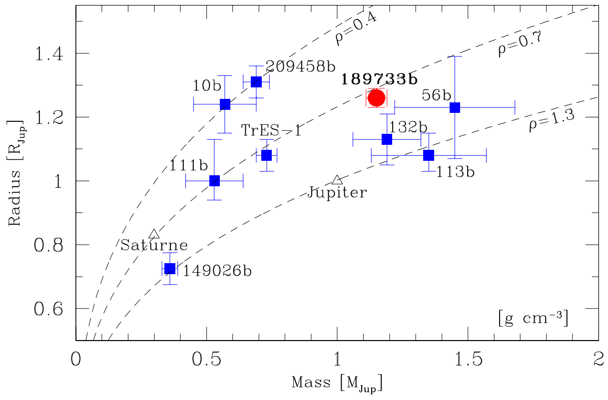

- Masses and radii:
  $\Longrightarrow$ density
- many similar to Saturn and Jupiter
- several less dense than Saturn and Jupiter
- inflated by heating by host star

Low densities $\Longrightarrow$ these planets are made of gas!

Transits

Occultation technique *very* difficult from ground $\Longrightarrow$ go to space!

NASA: Kepler spacecraft, launch 2009-03-07,

Continuous photometry of 145000 stars in 12° field of view using 45 CCDs with 2200 × 1024 pixel each (95 Megapixel)

Reaches 20 ppm at 12 mag in 6.5 h integration

(Earth-like planet: ~100 ppm)

2nd data release: 2011 February 2: 1235 candidates around 997 host stars

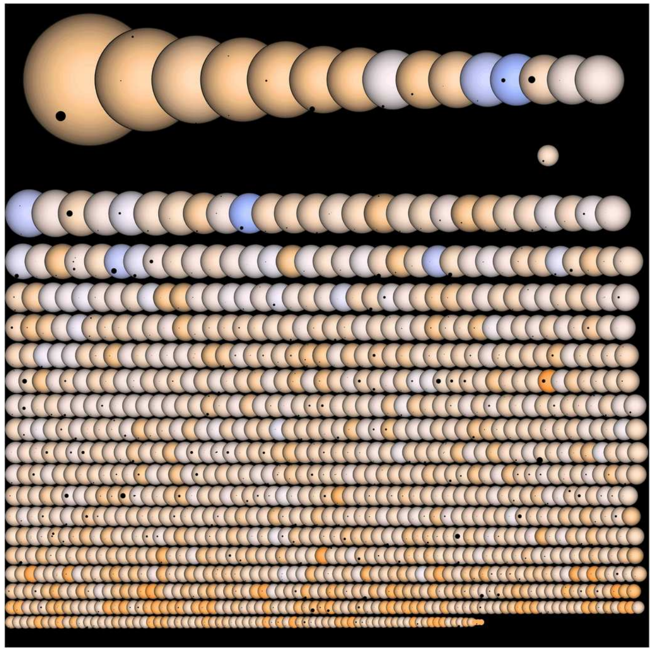

NASA/Rowe

Kepler's 1235 candidates; movie time: `planets/orrery810px.mov`

Results

Kepler: *candidates*. Many still require independent confirmation (=are not yet *discoveries*)

As of 4 July 2011, 564 extrasolar planets were known.

Lots of information can be found at `http://www.exoplanet.eu/` and `http://exoplanets.org`

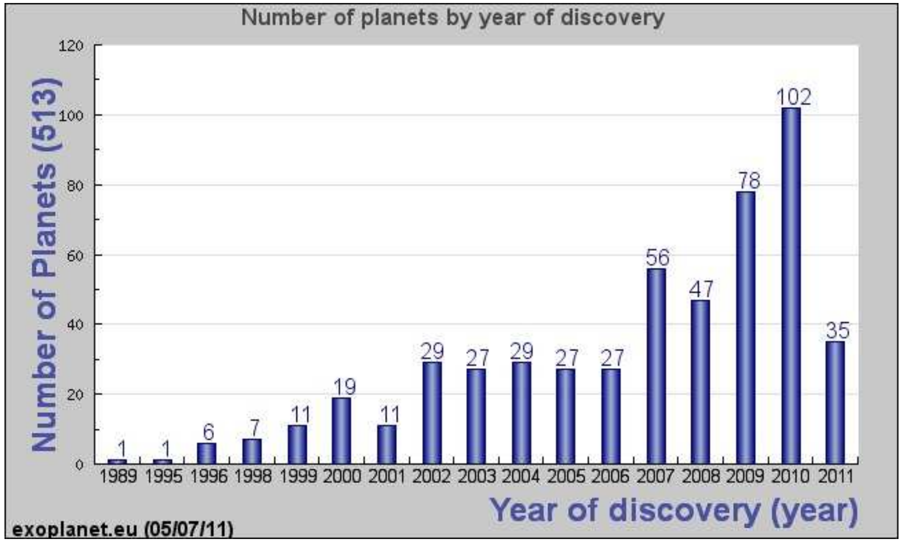

`http://www.exoplanet.eu`

Results

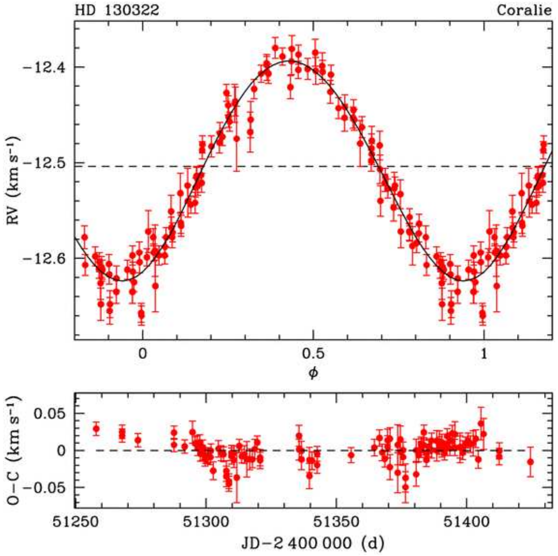

Example: Changing radial velocity of HD 130322 results in discovery of Jupiter-mass planet (Udry et al., 2000).

Here: velocity amplitude: $115\,\mathrm{m\,s^{-1}}$.

Radial velocity = velocity along our line of sight.

Results

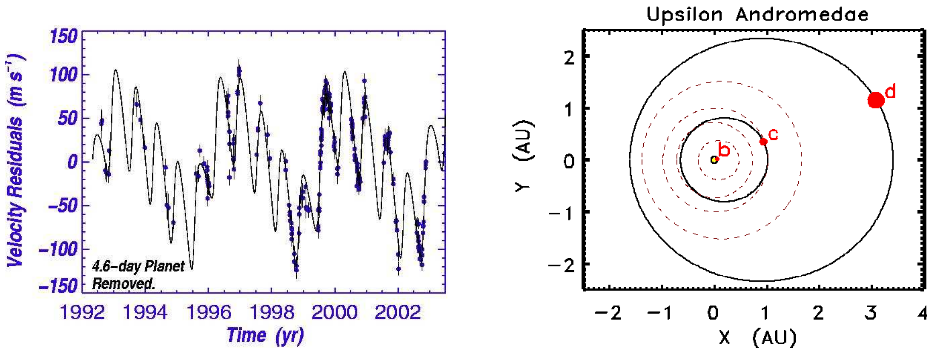

G. Marcy/UC Lick

Velocity signature and orbits of the three planets around υ Andromedae.

Results: Mass limits

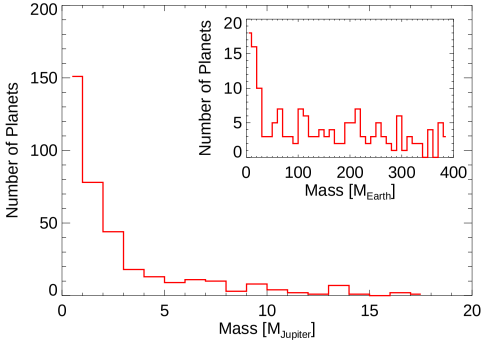

- Except for transits: Only mass function can be directly derived:

$$f(M) = \frac{M_\mathrm{p}\,(\sin i)^3}{\left(1+\frac{M_\mathrm{s}}{M_\mathrm{p}}\right)^2} = \frac{P\,K_s^3}{2\pi G} \qquad (11.3)$$

- mass of the star M_s from spectroscopy $\Longrightarrow M_\mathrm{p}\sin i$, i.e., lower limit to the planet's mass M_p; inclination remains indetermined
- Many (most!) Planets found have $M_\mathrm{p}\sin i > M_{♃}$ ($M_{♃} = 318\,M_\oplus$)

Selection effect: large $M \Longrightarrow$ larger velocity amplitude $\Longrightarrow$ easier to detect!

So, the fact that we have not seen any Earth-like planets does not mean that they do not exist, just that we cannot detect them yet. Smallest mass found so far: 1.94 $M_\oplus$ (Gliese 581e)

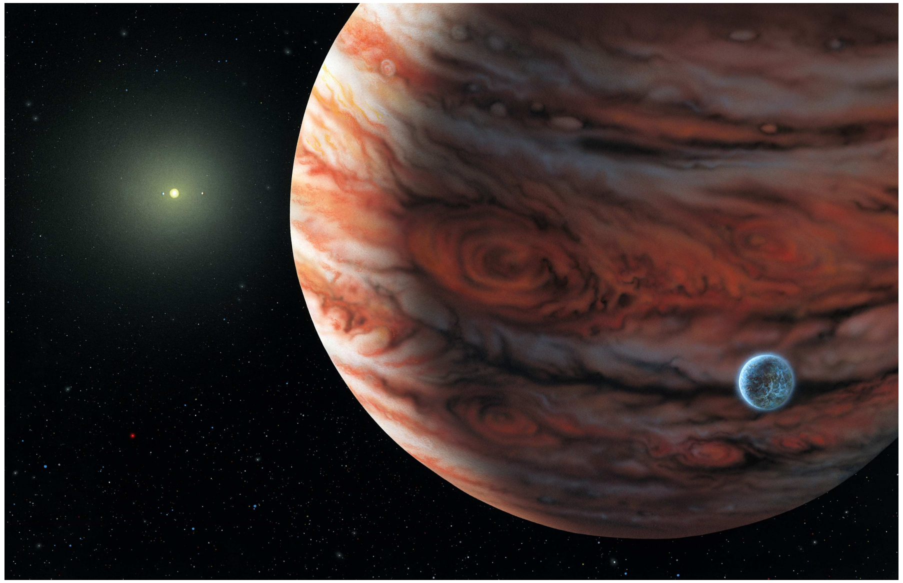

ESA press release, copyright 2002 Lynette Cook, `http://extrasolar.spaceart.org/`.

Jupiter-sized planet plus minor planets (left: detected, Jupiter-scale planet, right: hypothetical planet) around 55 Cancri.

Results: Semimajor Axis

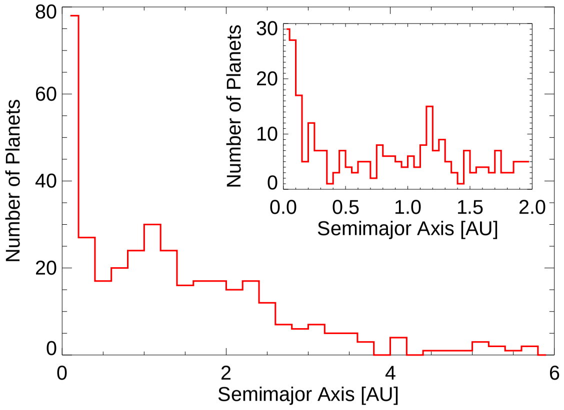

Most planets found are close to companion star!

Selection effect: small $a \Longrightarrow$ short period

$\Longrightarrow$ detectable in small amount of time (years, not decades)

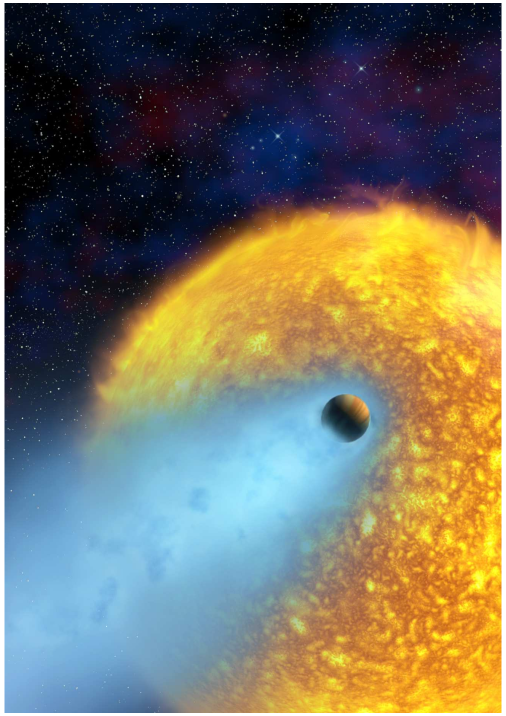

Jupiter-scale planets close to stars: “hot Jupiters”

e.g., HD 209458b, only 7 Million km from star: planet is evaporating (HST spectroscopy: mass loss is $10^7\,\mathrm{kg\,s^{-1}}$)!

ESA

Results: Period

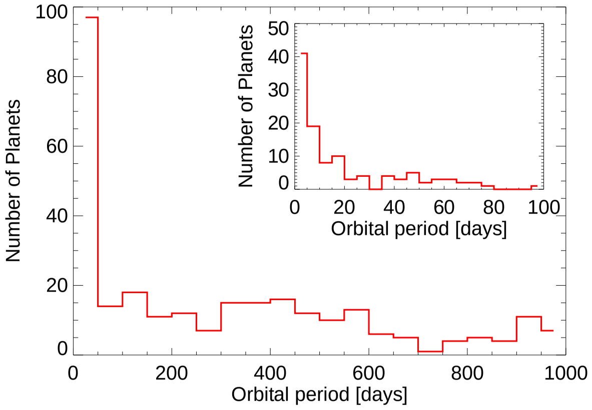

Most planets found in short orbits!

Statistics is direct consequence of the selection effect of the previous slide: short period planets are detectable during typical durations of observing runs. . .

Results: Eccentricity

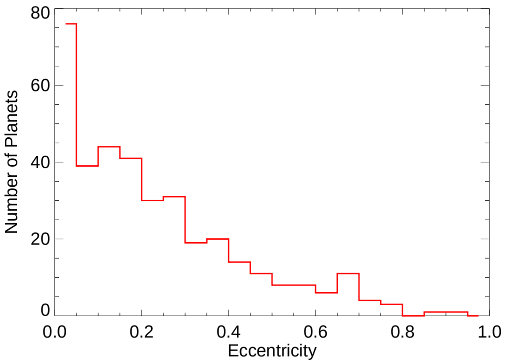

Many planets are in eccentric orbits!

different from solar system!

Might be selection effect due to our existence:

Jupiter in eccentric orbit in our solar system

$\Longrightarrow$ strong disturbances of Earth's orbit $\Longrightarrow$ no life!

So, in some sense Copernican principle does *not* always seem to hold!

D.M.Hardy / PPARC

But not all is bleak – HD 70642 ($d = 90$ ly): discovered by Hugh Jones (Liverpool John Moores University): Jupiter mass planet at 3 AU from solar-like star in circular orbit

$\Longrightarrow$ stable Earths are possible.

Habitable Zone

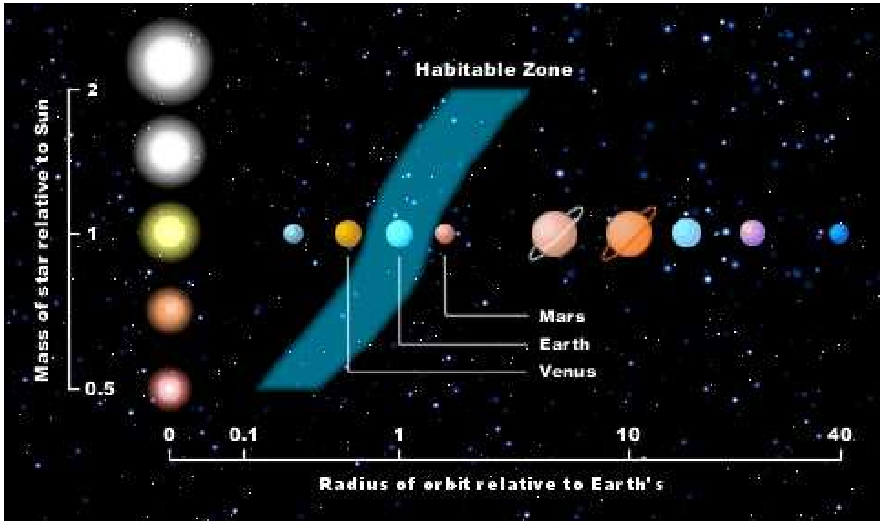

Habitable Zone

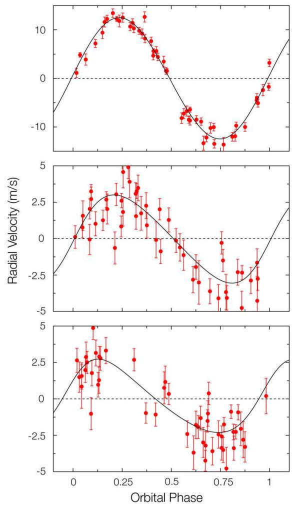

Observed Velocity Variation of Gliese 58

- Gliese 581: red dwarf star cooler and smaller than sun
- three planets, all of low mass
- Gliese 581c: $M_p \sin i = 5M_\oplus$ lowest mass limit found yet
- Gliese 581c orbits within habitable zone ($a = 0.073$ AU, $e = 0.16$)

Kepler: ~50 candidates in habitable zone

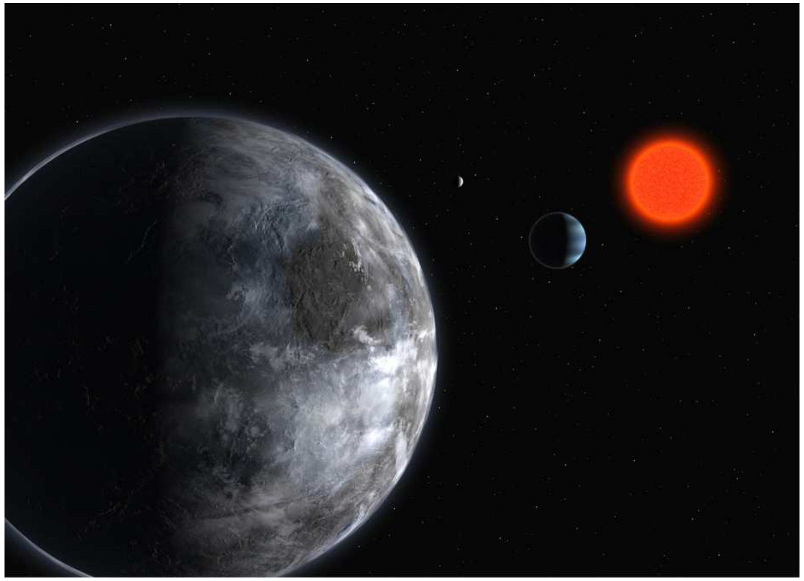

The Planetary System in Gliese 581
(Artist's Impression)

ESO Press Photo 22a/07 (25 April 2007)

Summary

Detections: of the 564 planets known to date (4.7.2011):

- 431 were discovered through Doppler motion, 133 are transiting
- 21 were discovered through imaging

Properties:

- Hot Jupiters: very close orbits (periods of few days, e.g. 51 Peg)
- Jupiters on very eccentric orbits (70 Vir)
- Jupiters on nearly circular orbits and long periods (e.g. 47 UMa)
- Planets with masses similar to Saturn
- Planets with masses similar to Neptune
- 45 planetary systems: 55 Cnc has five planets
- Gliese 581: planet in the habitable zone?
- CoRoT 7b = Super-Earth: mass of 4.8$M_\oplus$
  density = 5.6 $\pm$ 1.3 g/cm^3

Stars: Formation

Optical View of B68 (ESO; VLT/FORS1)

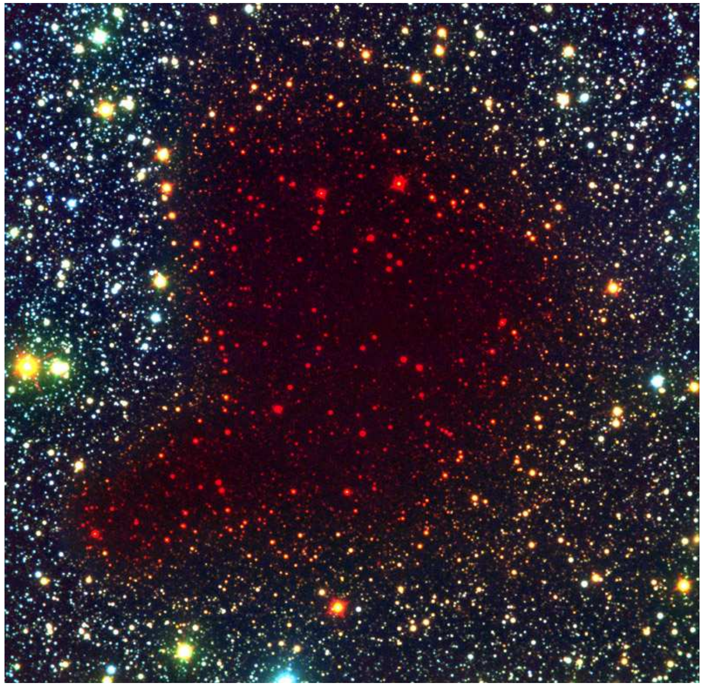

IR View of B68 (ESO; VLT/FORS1 + NTT/SOFI)

Stellar Birth

Stars are born in “Giant Molecular Clouds”

Typical GMC parameters (e.g., Orion):

- large clouds: typical diameters 50–100 pc
- contain lots of molecular gas (H_2, CO, alcohol,. . .).
- typical temperatures: 10–20 K (coolest regions in the interstellar medium)
- typical particle densities $n \sim 10^6$–10^{10} cm^{-3}

Stars are born in groups out of collapsing Molecular Clouds.

Collapse triggered, e.g., by collisions of clouds or shocks caused by nearby supernovae.

Stellar Birth

Criterion for collapse: Cloud is instable, i.e., gravitation is stronger than thermal pressure.

In terms of thermal and gravitational energies, this means

$$\frac{3}{2}\frac{M}{m_\mathrm{p}}kT - \frac{3}{5}\frac{GM^2}{R} \leq 0 \tag{12.1}$$

which can be expressed as

$$\frac{M}{R} \geq \frac{5}{2}\frac{kT}{Gm_\mathrm{p}} \quad \text{or} \quad \frac{4\pi}{3}\rho R^2 \geq \frac{5}{2}\frac{kT}{Gm_\mathrm{p}} \tag{12.2}$$

$\Longrightarrow$ Depends on R, collapse thus possible for

$$R > R_\mathrm{J} = \sqrt{\frac{15kT}{8\pi G m_\mathrm{p}\rho}} \sim \sqrt{\frac{kT}{Gm_\mathrm{p}\rho}} \tag{12.3}$$

where R_J is called the Jeans radius.

Stellar Birth

Plugging in typical typical numbers, i.e., $T \sim 50$ K, particle density $n = 10^5$ H-atoms cm^{-3} (=a mass density of $\rho = nm_\mathrm{p} \sim 1.7 \times 10^{-9}$ g cm^{-3}) gives $R_\mathrm{J} \sim 0.2$ pc.

For a given Jeans radius, the mass within R_J is the Jeans mass

$$M_\mathrm{J} \sim \frac{4\pi}{3} R_\mathrm{J}^3 \rho$$

. . . which has typical values of 50–100 $M_\odot$, i.e., larger than one star!

In reality things are more complicated: ISM contains magnetic fields

$\Longrightarrow$ Particle motion $\perp$ B-field lines difficult

$\Longrightarrow$ stops gas from collapsing.

This is good since Jeans formalism alone predicts too strong star formation.

$\Longrightarrow$ Need star formation with magnetic fields

See Shu et al. (1987, Annual Reviews of Astronomy and Astrophysics 25, 23) for the gory details.

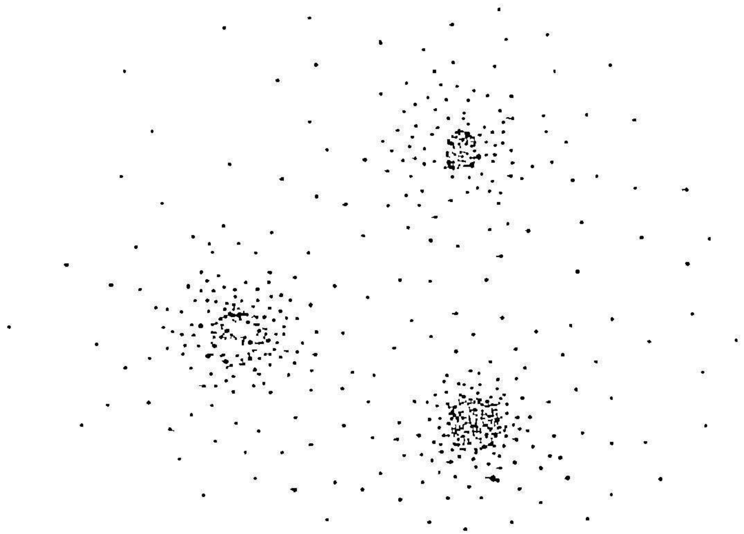

a

Shu et al. (1987, ARAA 25, 23, Fig. 7)

Stellar mass cores form from fragmentation of larger pieces.

Note: fragmentation only along B-field lines.

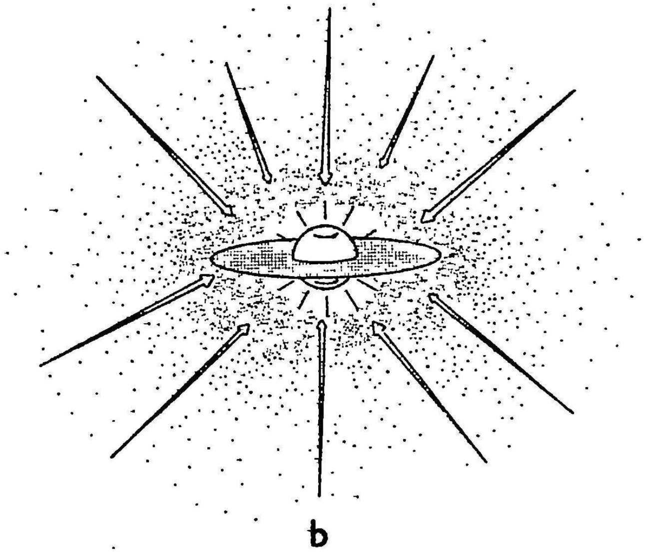

b

Shu et al. (1987, ARAA 25, 23, Fig. 7)

Protostar forms with surrounding disk (“inside out collapse”) once core hot enough to allow fusion ($T > 10^6$ K)

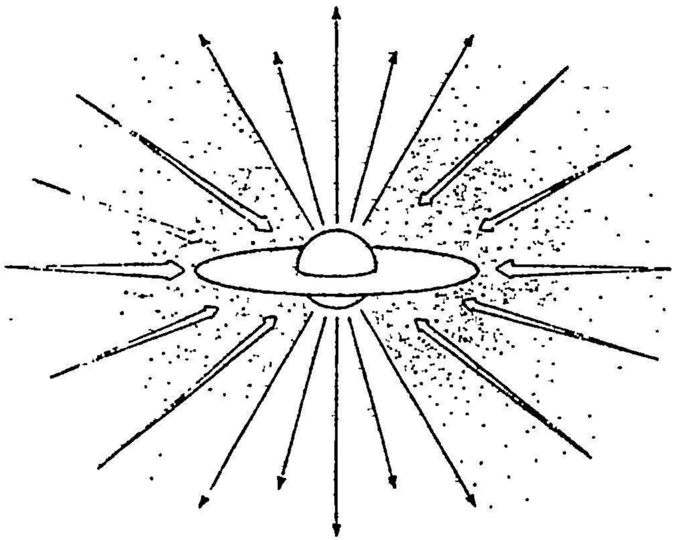

c

Shu et al. (1987, ARAA 25, 23, Fig. 7)

Stellar wind forms bipolar outflow

Orion (Bayer’s Uranometria; image ⓒUSNO)

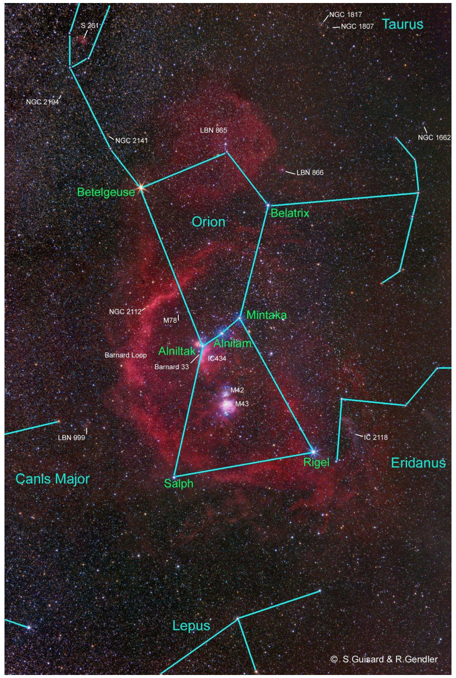

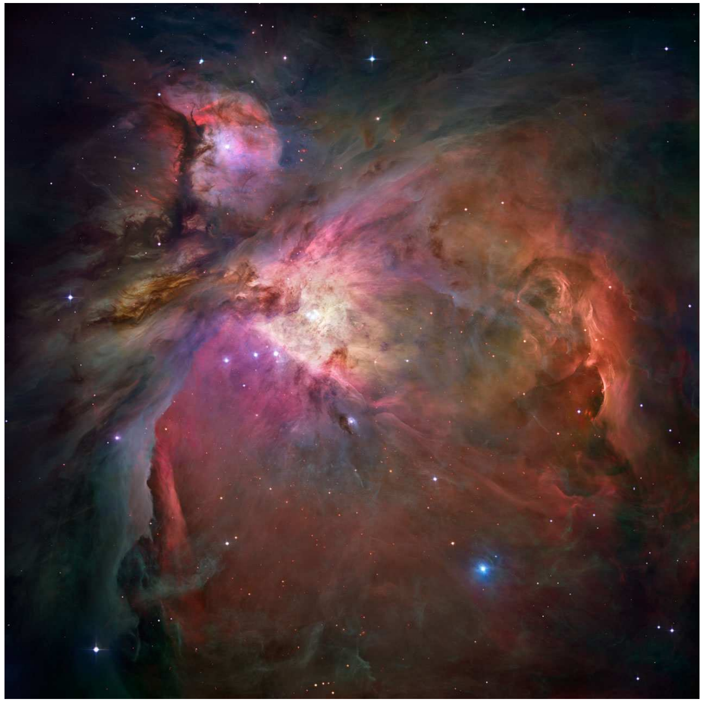

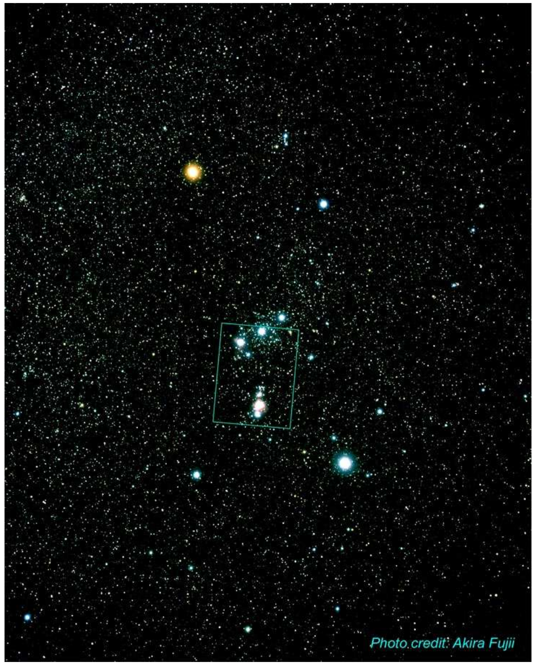

Movie Time:

`movies/starformation_movies/orion_zoom.mo`

from

`http://hubblesite.org/newscenter/archive/`

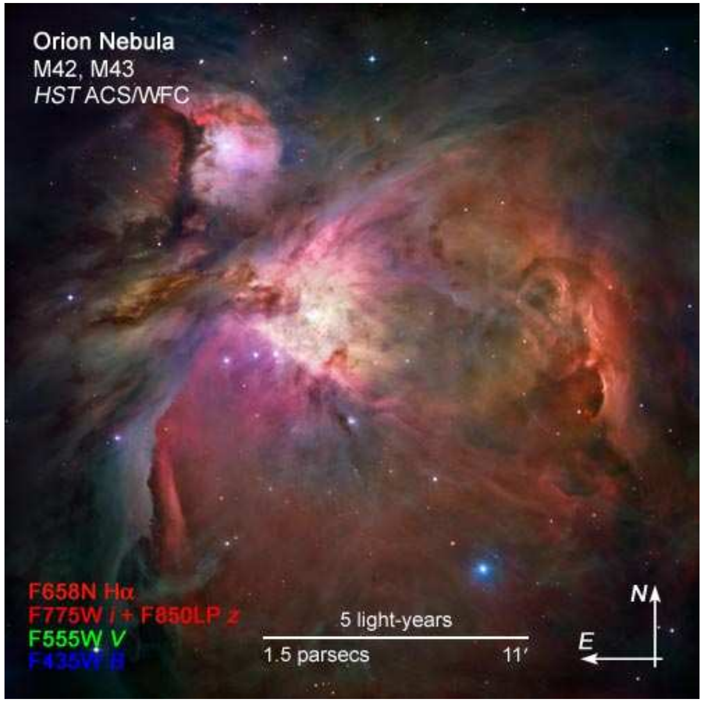

Orion Nebula; R. Gendler

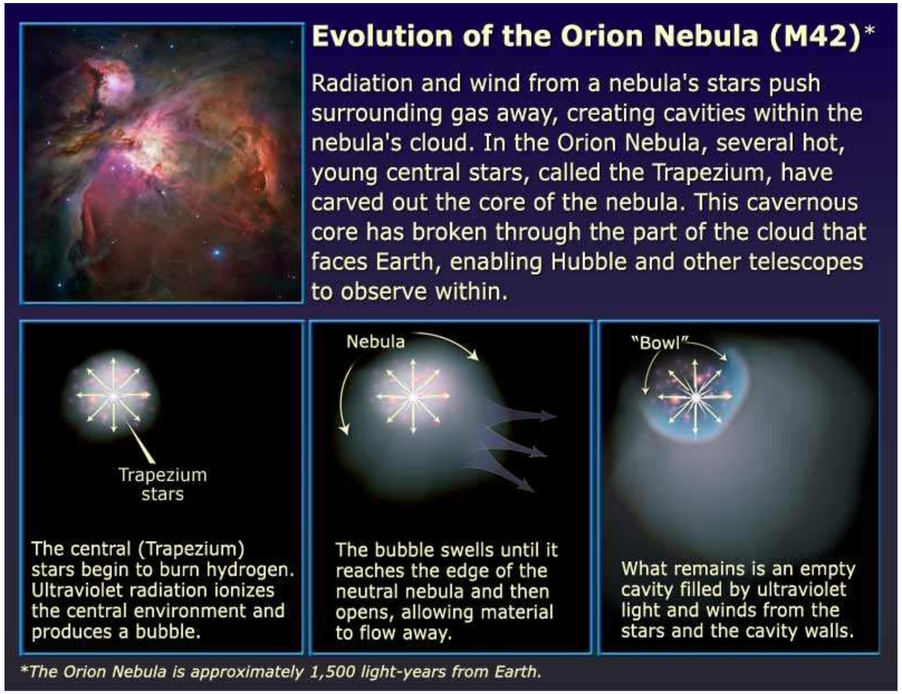

Evolution of the Orion Nebula (M42)*

Radiation and wind from a nebula's stars push surrounding gas away, creating cavities within the nebula's cloud. In the Orion Nebula, several hot, young central stars, called the Trapezium, have carved out the core of the nebula. This cavernous core has broken through the part of the cloud that faces Earth, enabling Hubble and other telescopes to observe within.

The central (Trapezium) stars begin to burn hydrogen. Ultraviolet radiation ionizes the central environment and produces a bubble.

The bubble swells until it reaches the edge of the neutral nebula and then opens, allowing material to flow away.

What remains is an empty cavity filled by ultraviolet light and winds from the stars and the cavity walls.

*The Orion Nebula is approximately 1,500 light-years from Earth.

STScI

Orion Nebula; R. Croman

Photo Credit: T. Rector (University of Alaska)

Eagle-nebula (M16)

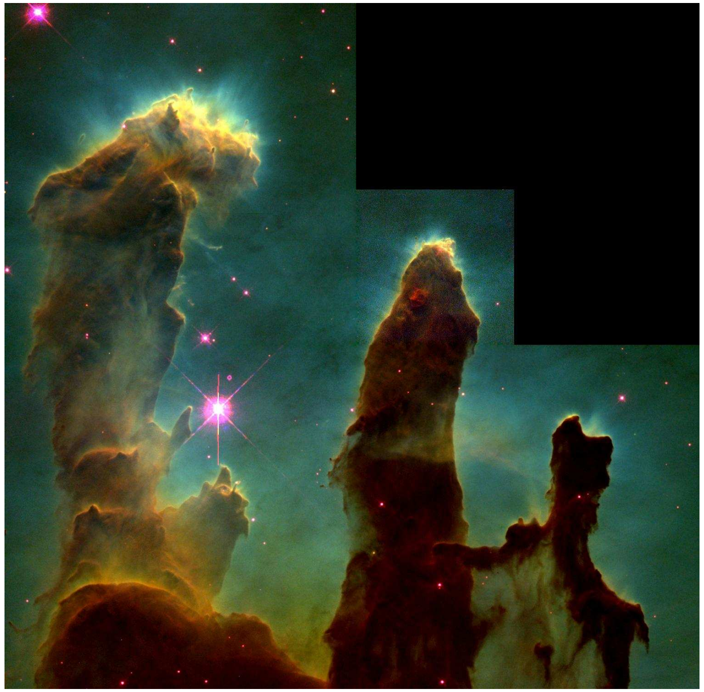

“pillars of creation” in Eagle Nebula (M16)

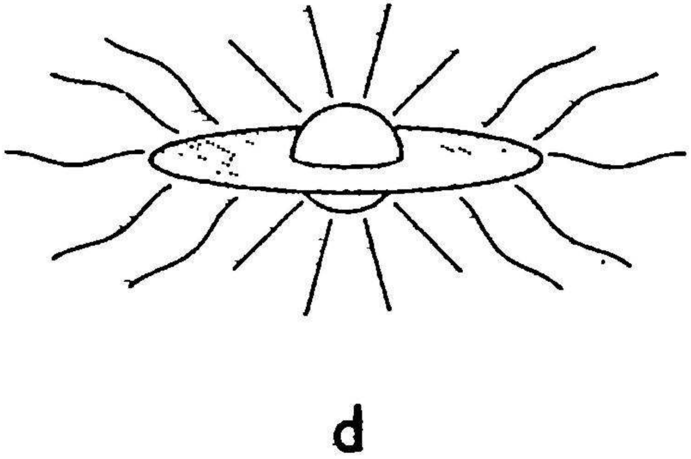

Shu et al. (1987, ARAA 25, 23, Fig. 7)

Star has reached zero age main sequence (ZAMS) plus circumstellar disk.
Some disks produce fast collimated outflows (**jets**): **Herbig Haro Objects**

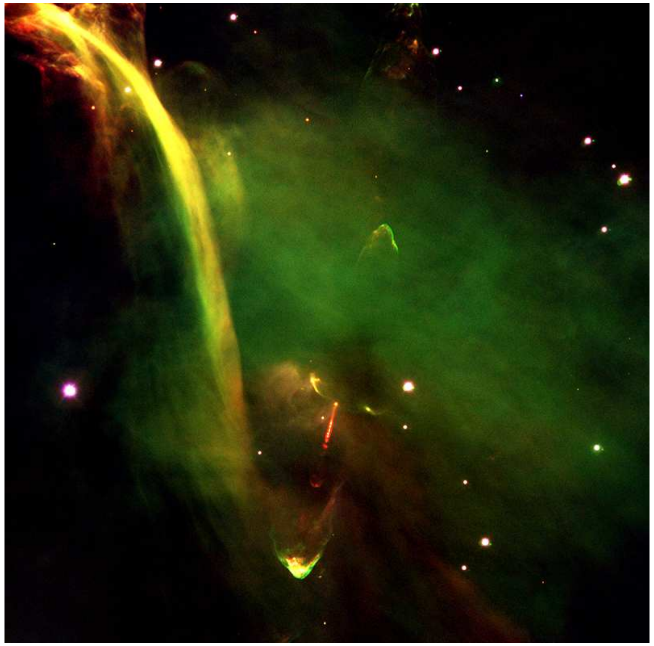

HH34 in Orion (ESO VLT KUEYEN/FORS2)

Herbig Haro Objects: **shocks** and **jets/outflows** produced during formation of stars.

Pleiades (R. Gendler; $d = 150\,\mathrm{pc}$, diameter: $5\,\mathrm{pc}$, 3000 stars

Once stars have formed, strong UV radiation removes residual dust (still seen as a **reflection nebula**) and an **open cluster** is formed.

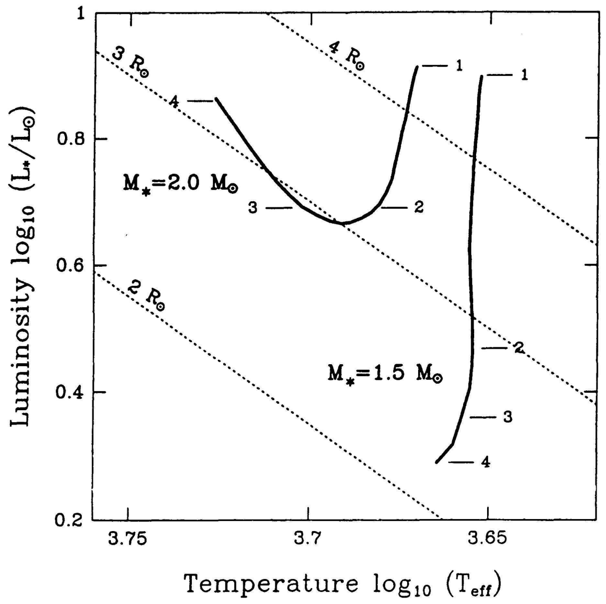

Palla & Stahler (1993, ApJ 418, 414; numbers are time in 10^6 years)

Stellar Evolution from protostar to ZAMS takes a few million years.

Zero Age Main Sequence

Once star has collapsed and nuclear fusion has started: zero age main sequence (ZAMS) is reached

The Main Sequence is the result of steady state fusion (“burning”) of hydrogen into helium in stellar centers.

. . . longest phase of stellar evolution (10 billion years for Sun)

Stellar structure defined by balance between pressure inwards due to gravitation and pressure outwards due to energy release (“hydrostatic equilibrium”).

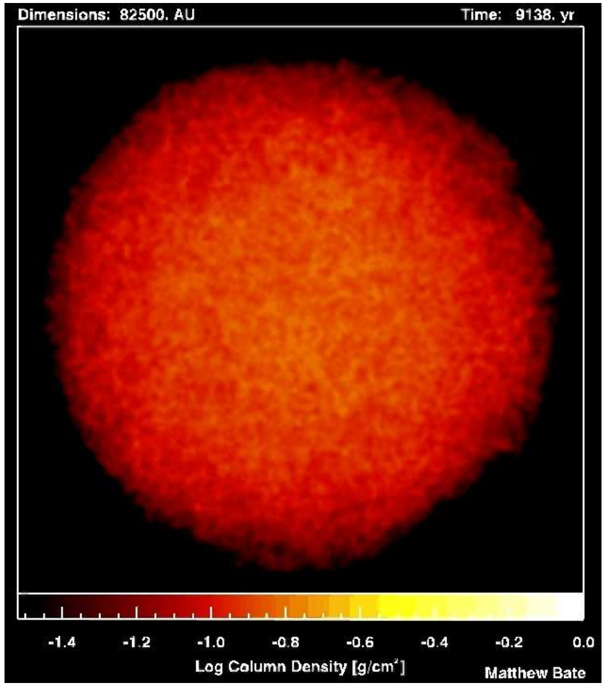

Movie time: `starformation_movies/cluster_formation_bate.avi`

Stars: Structure and Evolution

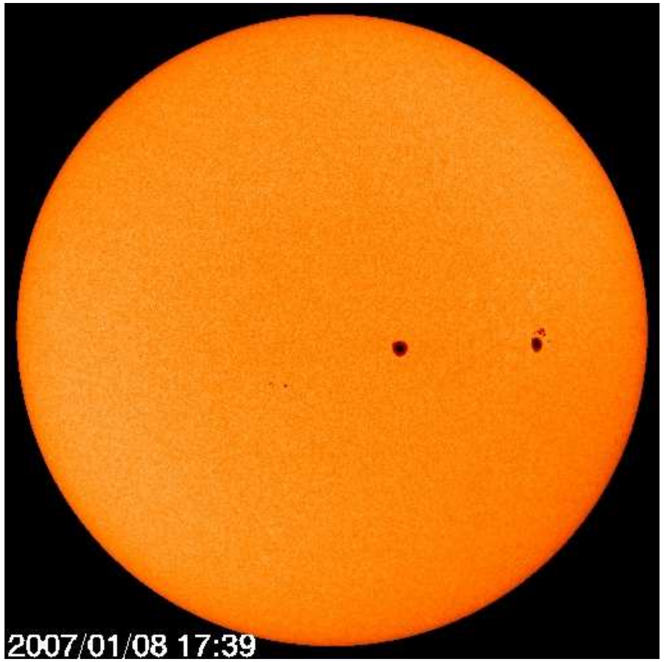

The Sun: A typical star (ESA/NASA SOHO)

Stellar Structure

The structure of stars is defined by a set of four coupled differential equations which express the basic conservation and transport quantities always encountered in physics:

1. Mass conservation
2. Momentum conservation (=hydrostatic equilibrium)
3. Energy conservation
4. Energy transport

and quantities expressing the physical properties of material, mainly:

1. Energy generation
2. Equation of state (=dependence of density of material on physical conditions)

Mass Conservation

Density stratification of a star is defined through mass conservation:

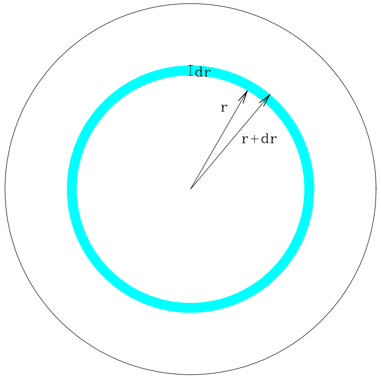

Define M_r as the mass contained within radius r:

$$M_r = \int_0^r 4\pi r^2 \rho(r)\,\mathrm{d}r \tag{13.1}$$

Thus the mass within a spherical shell is

$$\mathrm{d}M_r = 4\pi r^2 \rho\,\mathrm{d}r \tag{13.2}$$

and therefore

$$\frac{\mathrm{d}M_r}{\mathrm{d}r} = 4\pi r^2 \rho \tag{13.3}$$

Hydrostatic Equilibrium

Pressure stratification of a star is defined through hydrostatic equilibrium:

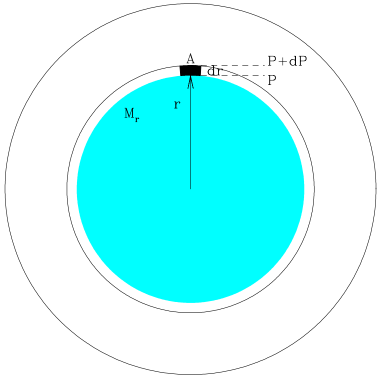

Force on area A by slab of gas of area $\mathrm{d}A$ and density ρ:

$$\mathrm{d}F_g = -\frac{GM_r \mathrm{d}m}{r^2} = -\frac{GM_r\rho}{r^2}\mathrm{d}A\,\mathrm{d}r \tag{13.4}$$

Bouyancy:

$$F_P = \mathrm{d}A(P(r+\Delta h) - P(r)) = \mathrm{d}A\Delta P \tag{13.5}$$

Balance of forces:

$$-\frac{GM_r\rho}{r^2}dA\,dr = dP\,dA \tag{13.6}$$

such that

$$\frac{\mathrm{d}P}{\mathrm{d}r} = -\rho(r)\frac{GM(r)}{r^2} \tag{13.7}$$

Energy Conservation

Temperature stratification of a star is defined through energy conservation:

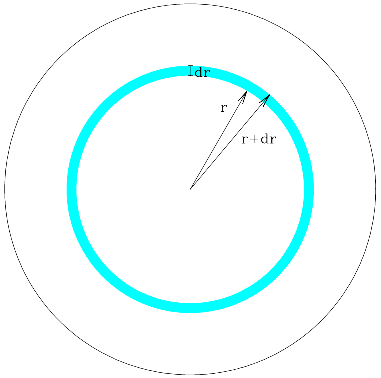

Let ϵ = energy production coefficient, i.e., the energy released per time and unit mass.

Luminosity produced within a spherical shell is

$$\mathrm{d}L_r = \epsilon \mathrm{d}M_r = 4\pi r^2 \rho\epsilon\,\mathrm{d}r \qquad (13.8)$$

and therefore

$$\frac{\mathrm{d}L_r}{\mathrm{d}r} = 4\pi r^2 \rho\epsilon \qquad (13.9)$$

Energy Transport

Energy is transported in stars by

- radiation
- convection
- conduction

In most stars, radiation and convection are important, conduction usually not.

Radiative Transport = diffusive process:

- radiation produced by nuclear fusion (γ-rays)
- mean free path l_{phot} of a photon in center of the Sun: few cm
- photons do random walk to the stellar surface absorbed by ions and reemitted
- number of "scatterings": $N = (R/l_{\text{phot}})^2$: e.g., $R_\odot = 700000\,\text{km}$: $N \approx 10^{20}$
- Diffusion theory:

$$\frac{\mathrm{d}T}{\mathrm{d}r} = -\frac{3}{4ac}\frac{\kappa(r)\rho(r)}{T^3}\frac{L(r)}{4\pi r^2} \qquad (13.10)$$

Energy Transport

Convection is much more difficult to deal with, no self-consistent hydrodynamical treatment, approximate (so called mixing-length) theory

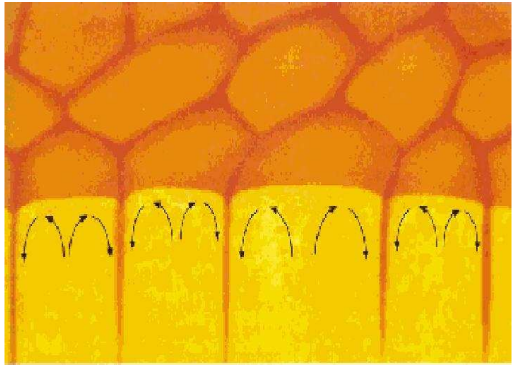

$$\frac{\mathrm{d}T}{\mathrm{d}r} = \left(1 - \frac{1}{\gamma}\right)\frac{T}{P}\frac{\mathrm{d}P}{\mathrm{d}r} \qquad (13.11)$$

Structure equations

Stellar structure governed by four coupled differential equations:

Mass structure
(mass conservation)

$$\frac{\mathrm{d}M}{\mathrm{d}r} = 4\pi r^2 \rho(r)$$

Pressure structure
(hydrostatic equilibrium)

$$\frac{\mathrm{d}P}{\mathrm{d}r} = -\rho(r)\frac{GM(r)}{r^2}$$

Temperature structure
(e.g. radiative transfer)

$$\frac{\mathrm{d}T}{\mathrm{d}r} = -\frac{3}{4ac}\frac{\kappa\rho(r)}{T^3}\frac{L(r)}{4\pi r^2}$$

Energy conservation

$$\frac{\mathrm{d}L}{\mathrm{d}r} = 4\pi r^2 \rho(r)\epsilon(r)$$

plus "equation of state" ($P = P(T, \rho)$), Opacities $\kappa(T, \rho, Z)$ = interaction of radiation with gas, energy generation ($\epsilon = \epsilon(T, \rho, Z)$),...

Stellar model: numerical solution of stellar structure equations.

Energy generation: Overview

Main sequence: Nuclear fusion of Hydrogen into Helium:

$$4\mathrm{p} \longrightarrow {}^4_2\mathrm{He} + E$$

How much energy is gained?

Particle physics: express mass as “rest energy equivalent” via $E = mc^2$

(and call it “mass”. . .); usually use energy units of MeV, 1 MeV $= 1.602 \times 10^{-13}$ J

$$\begin{array}{lr} \text{mass of 4 protons } (4 \times 938\,\text{MeV}): & 3752\,\text{MeV} \\ -\ \text{mass of } {}^4_2\text{He}: & 3727\,\text{MeV} \\ \hline \text{mass defect } \Delta mc^2: & 25\,\text{MeV} \end{array}$$

In the fusion of hydrogen to helium, 0.7% of the available rest mass energy is converted to energy.

Two main burning cycles: proton-proton chain and the CNO cycle.

Energy generation: Proton-Proton chain

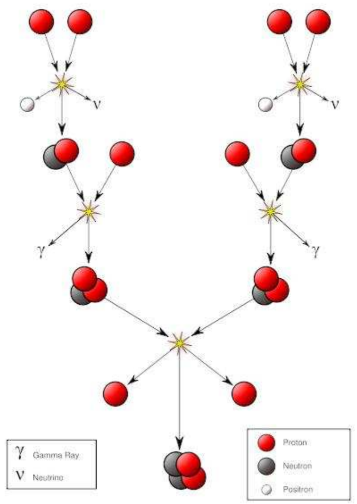

For moderate central temperatures, He is produced using the proton-proton chain.

First, two protons create a deuteron:

$$^1\mathrm{H} + {}^1\mathrm{H} \longrightarrow {}^2\mathrm{H} + \mathrm{e}^+ + \nu_\mathrm{e} \qquad (13.12)$$

This process is slow (happens once for a nucleon per 10^{10} years)

Then an additional proton is attached:

$$^2\mathrm{H} + {}^1\mathrm{H} \longrightarrow {}^3\mathrm{He} + \gamma \qquad (13.13)$$

and two helium nuclei can form an α-particle:

$$^3\mathrm{He} + {}^3\mathrm{He} \longrightarrow {}^4\mathrm{He} + 2\,{}^1\mathrm{H} \qquad (13.14)$$

This is the so called pp I-cycle, minor variations of the theme exist (pp II, pp III cycles), but pp I dominates.

pp chain dominates for $T \lesssim 2 \times 10^7$ K, $\epsilon_\mathrm{pp} \propto T^5$; Sun: 98.4%.

Energy generation: CNO cycle

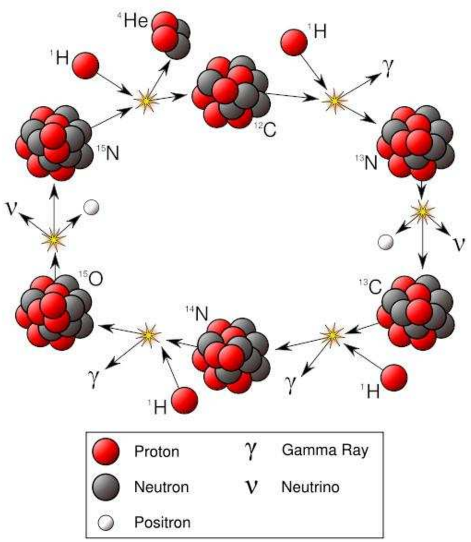

The CNO cycle (Bethe-Weizsäcker-cycle) requires the presence of C, N, and O isotopes as catalysts.

CNO cycle has slightly smaller energy release than pp-cycle because of higher neutrino losses.

Reaction $^{14}\mathrm{N} + \mathrm{p} \longrightarrow {}^{15}\mathrm{O} + \gamma$ is th slowest reaction (one million years).

CNO cycle dominates above 2×10^7 K, $\epsilon_\mathrm{CNO} \propto T^{17}$;

Sun: 1.6%.

Wikipedia

Stellar Evolution

Principle:

1. Construct stellar model by solving equations of stellar structure for given radial abundances.
2. Evaluate change in elemental abundances as a function of radius based on the local fusion processes.
3. Change abundances appropriately for a time step Δt.
4. goto step 1

We start with looking at models of the Sun in detail and then take a look at typical stellar evolution paths.

Characteristic Timescales

Main sequence: Hydrogen burning at the center.

Evolution timescale dominated by the nuclear timescale = timescale needed to use the fuel in the center of the star.

According to simulations, this is ~10% of the available Hydrogen.

Since 0.7% of $M_{\text{core}}c^2$ converted into He, the nuclear timescale is

$$t_{\text{n}} = \frac{0.007 \cdot 0.1 M c^2}{L} = \frac{M/M_\odot}{L/L_\odot} \cdot 10^{10}\,\text{years} \tag{13.15}$$

A second important timescale is the timescale the star would need to radiate its stored thermal energy: thermal timescale.

Roughly given as

$$t_{\text{t}} = \frac{0.5 G M^2/R}{L} = \frac{(M/M_\odot)^2}{(R/R_\odot)(L/L_\odot)} \cdot 2\times 10^7\,\text{years} \tag{13.16}$$

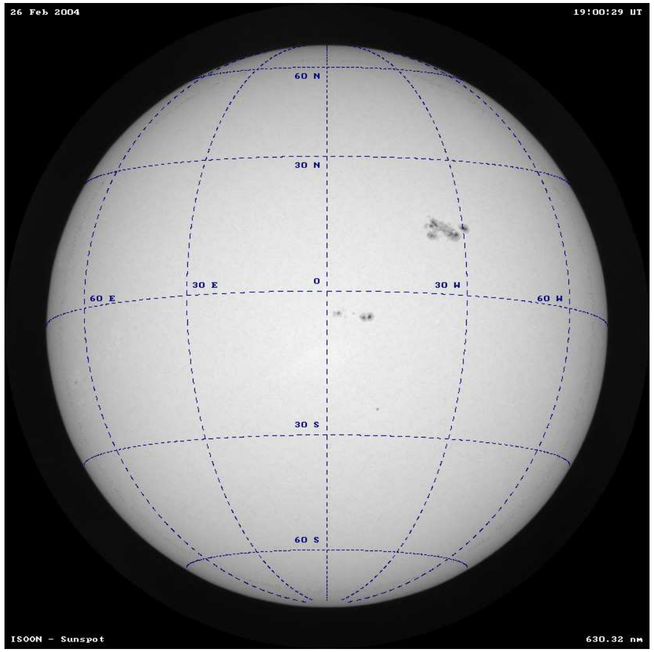

The Sun

Solar Structure

Based on observations of

- Solar Mass: 1 $M_\odot = 1.997\times10^{30}$ kg $= 1.997\times10^{33}$ g
- Solar Luminosity: 1 $L_\odot = 3.846\times10^{26}$ W $= 3.846\times10^{33}$ erg s^{-1}
- age: $t = 4.5\times10^9$ yrs
- Solar chemical composition (=elemental abundances) at the surface: 73.81% H, 24.85% He, 1.34% metals (by mass)

it is possible to use the equations of stellar structure to determine a model for the structure of the Sun, i.e., M_r, L_r, $\rho(r)$, $T(r)$, abundances(r) starting with a homogenous model and allow for 4.5 Gyrs of evolution.

Solar Structure

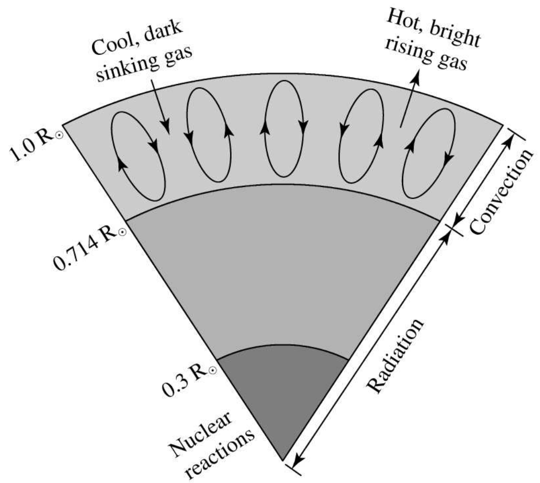

central conditions in the sun:

- $T_{\text{c}} = 1.57\times10^7$ K
- $P_{\text{c}} = 2.34\times10^{16}$ N m^{-2}
- $\rho_{\text{c}} = 1.53\times10^5$ kg m^{-3}
- Hydrogen fraction:
  $X = 0.34$ (by mass)
- Helium fraction:
  $Y = 0.64$ (by mass)

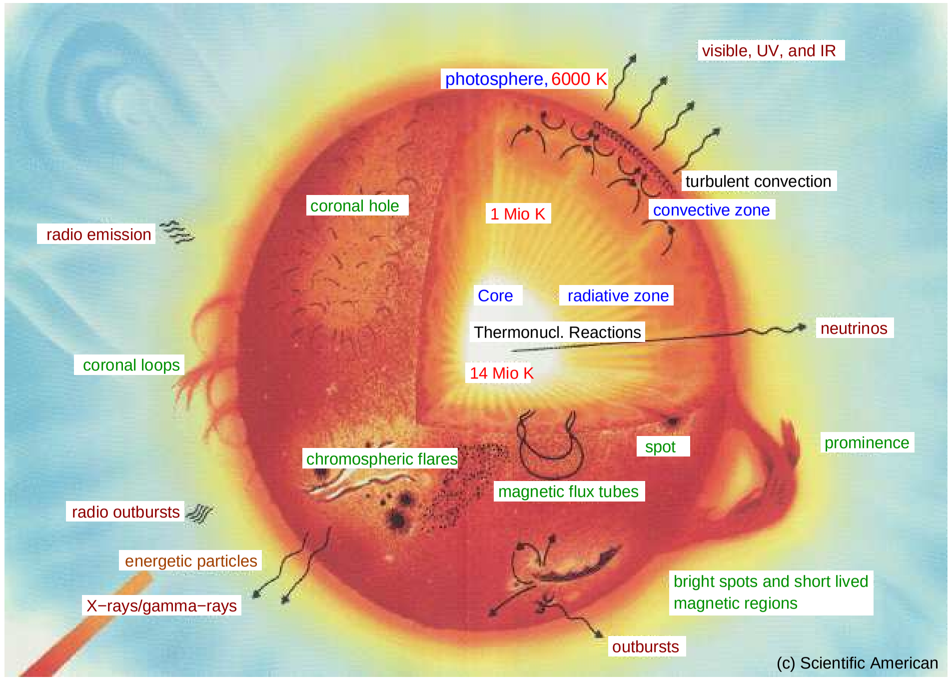

(c) Scientific American

Standard Solar Model

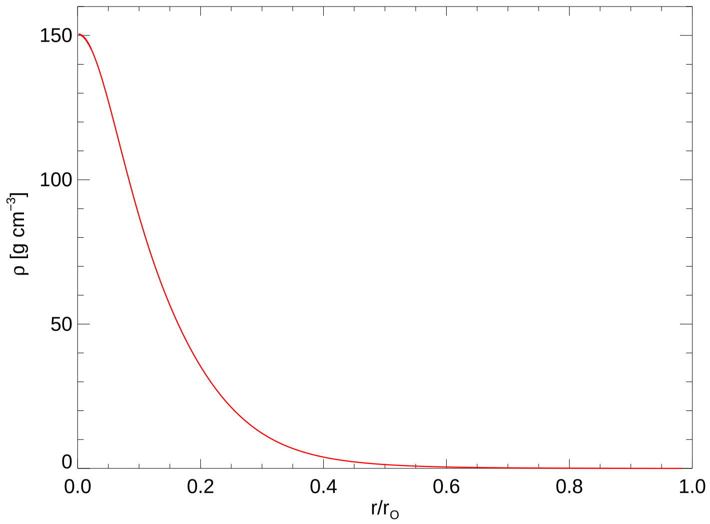

Standard solar model of Bahcall & Serenelli (2005, ApJ 626, 530)

Standard Solar Model

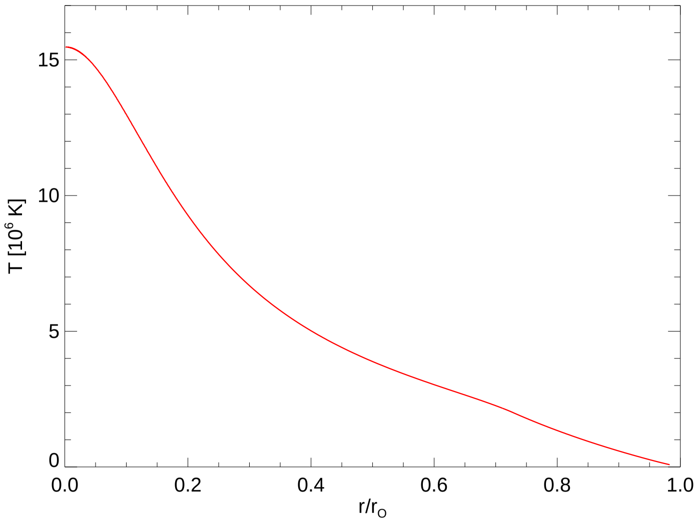

Standard solar model of Bahcall & Serenelli (2005, ApJ 626, 530)

Standard Solar Model

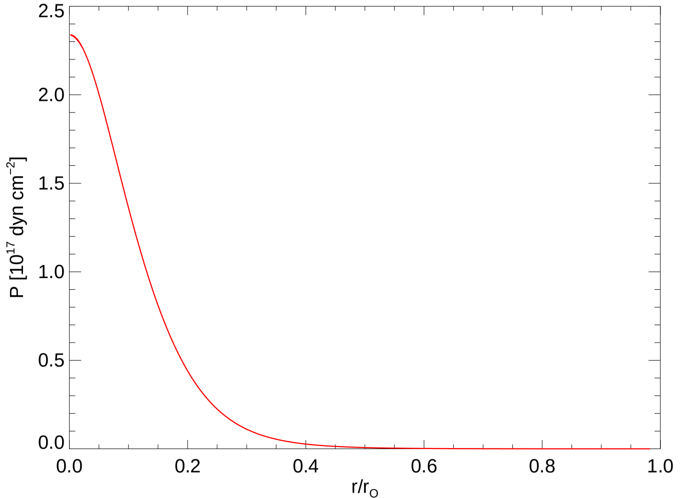

Standard solar model of Bahcall & Serenelli (2005, ApJ 626, 530; 1 dyn $= 10^{-5}$ N, 1 dyn cm^{-2} $=$ 0.1 Pa)

Standard Solar Model

Standard solar model:

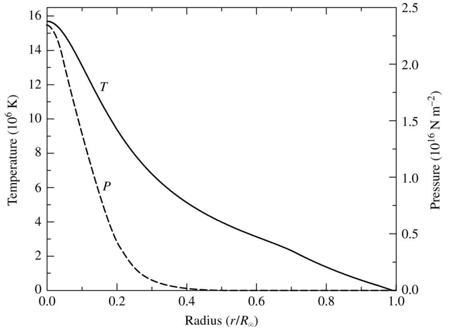

Temperature & pressure profile

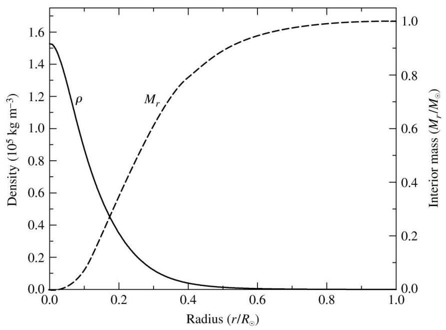

Density & interior mass profile

(Carroll & Ostlie)

Standard Solar Model

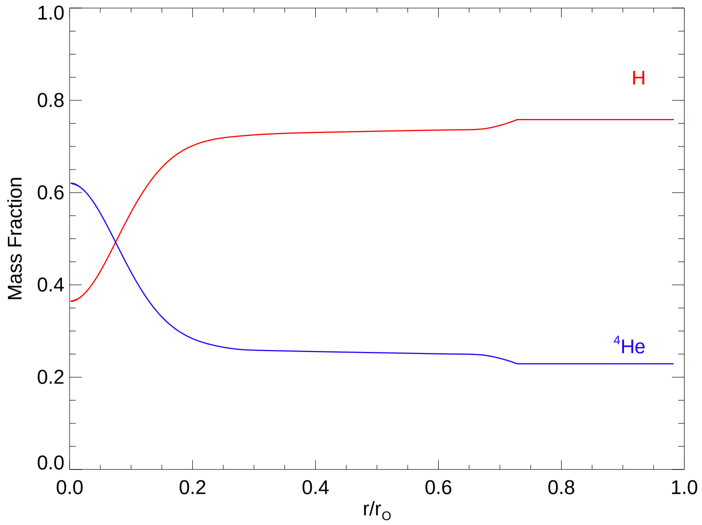

Standard solar model of Bahcall & Serenelli (2005, ApJ 626, 530)

Standard Solar Model

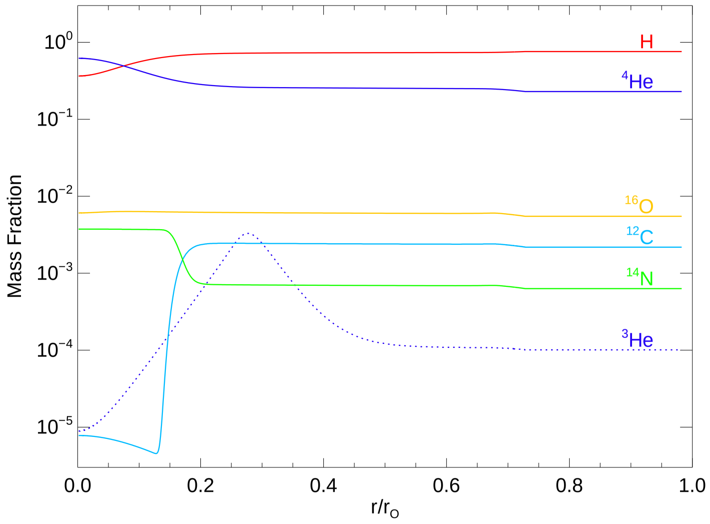

Standard solar model of Bahcall & Serenelli (2005, ApJ 626, 530)

Solar Evolution: Luminosity

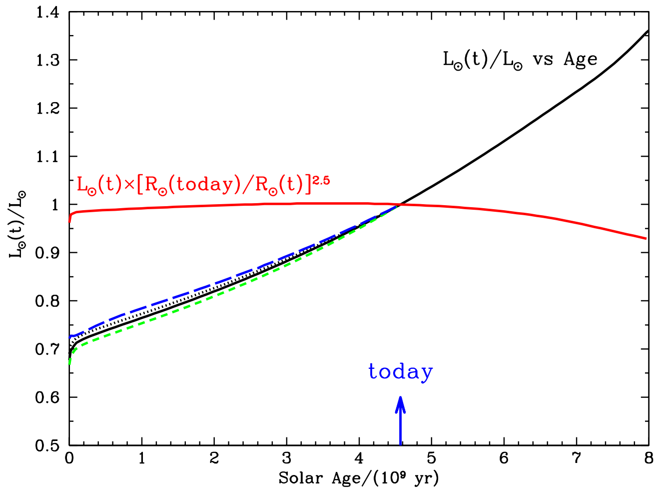

Bahcall, Pinsonneault & Basu (2001, ApJ 555, 990)

Solar Evolution: Radius

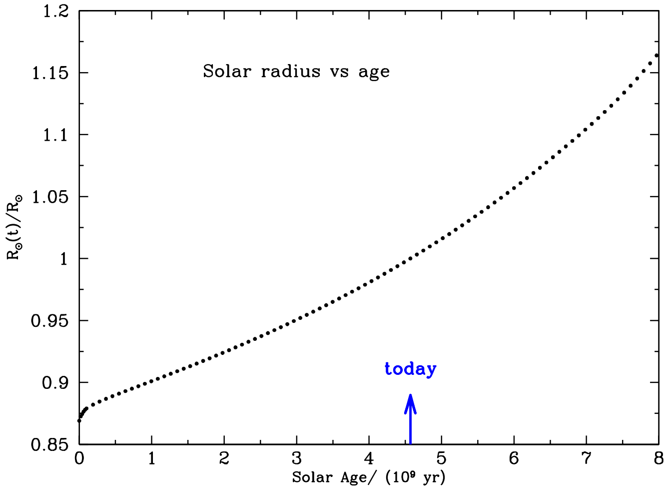

Bahcall, Pinsonneault & Basu (2001, ApJ 555, 990)

Solar Evolution: Energy Generation

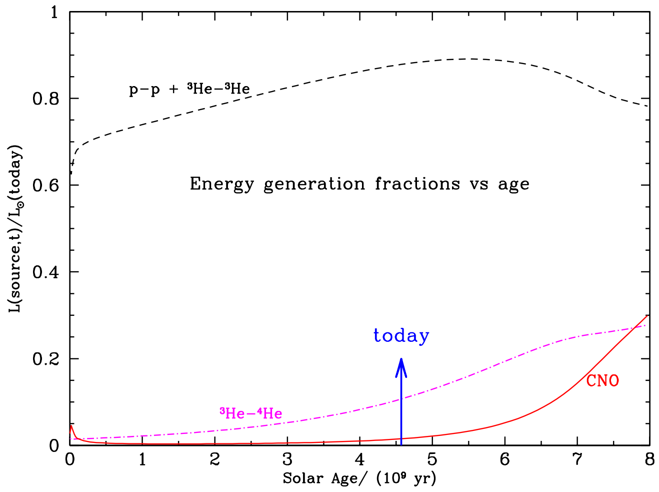

Bahcall, Pinsonneault & Basu (2001, ApJ 555, 990)

Solar Evolution: Center

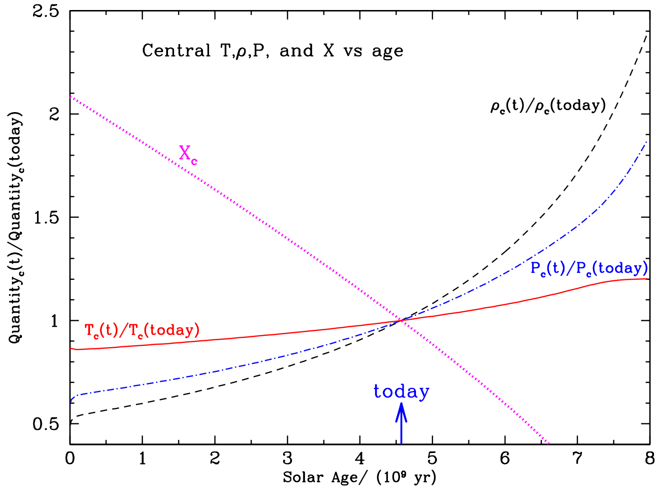

Bahcall, Pinsonneault & Basu (2001, ApJ 555, 990; X_c is the central H fraction)

Solar Neutrinos

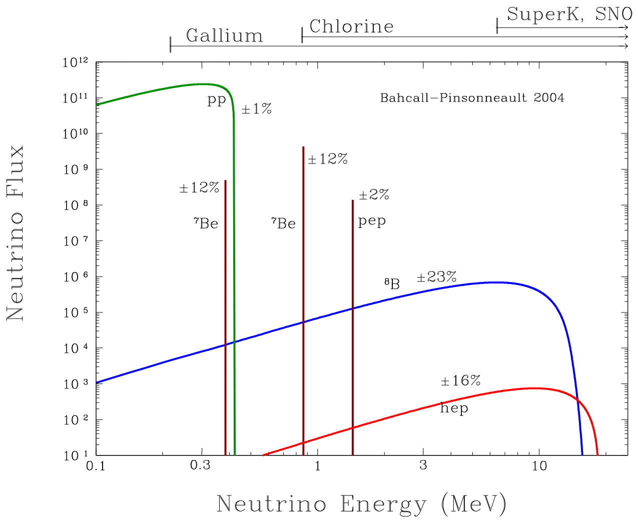

after Bahcall

The solar model predicts a solar neutrino spectrum that can be compared with Earth based measurements. This is the most direct test of theory of stellar structure known.

Problem: Neutrinos are difficult to detect since their interaction cross section is *very small*
$\Longrightarrow$ large detectors are needed.

The first neutrino experiment in the Homestake mine (J. Davis et al., 1968ff.).

Based on reaction

$$\nu_e + {}^{37}\mathrm{Cl} \longrightarrow {}^{37}\mathrm{Ar} + \mathrm{e}^-$$

Use Chlorine in large tetrachloroethylene tank (615 T), detect Ar with radiochemical methods.

Sensitive for electron neutrinos at energies above $\sim$0.8 MeV, which are rare.

Expected rate: 8.5 ± 1.9 SNU

Detected rate: 2.6 ± 0.2 SNU

1 SNU: 10^{-37} captures target atom^{-1} s^{-1}.

Brookhaven National Laboratory

Solar Neutrinos

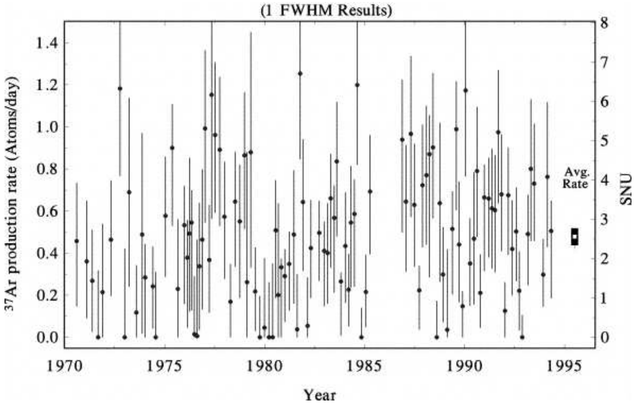

Cleveland et al. (1998, ApJ 596, 505; a total of 875 ^{37}Ar atoms were detected in the experiment, 766 of which were solar)

Low flux from early Homestake runs was confirmed in the early 1990s by Kamiokande.

Solar Neutrino Problem: Solar neutrino flux is $\sim$ 1/3 of predicted neutrino flux.

Most particle physicists believed that reason for the solar neutrino problem is that the standard solar model is wrong. They were wrong.

Solar Neutrinos

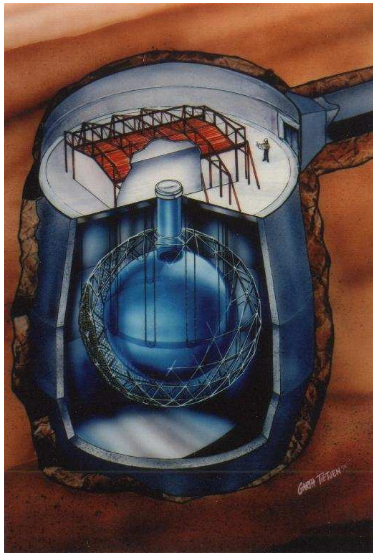

Sudbury Neutrino Observatory: uses 1000 T of heavy water, i.e., D_2O, 2000 m below ground.

Possible neutrino reactions:

charged current: $\nu_e + D \rightarrow \mathrm{p} + \mathrm{p} + \mathrm{e}^- - 1.442\,\mathrm{MeV}$

neutral current: $\nu + D \rightarrow \mathrm{p} + \mathrm{n} + \nu - 2.224\,\mathrm{MeV}$

elastic scattering: $\nu + \mathrm{e}^- \rightarrow \nu + \mathrm{e}^- - 2.224\,\mathrm{MeV}$

The neutral current reaction is sensitive to *any* flavor of neutrino.

SNO detects $\sim$5000 neutrino events per year.

courtesy SNO

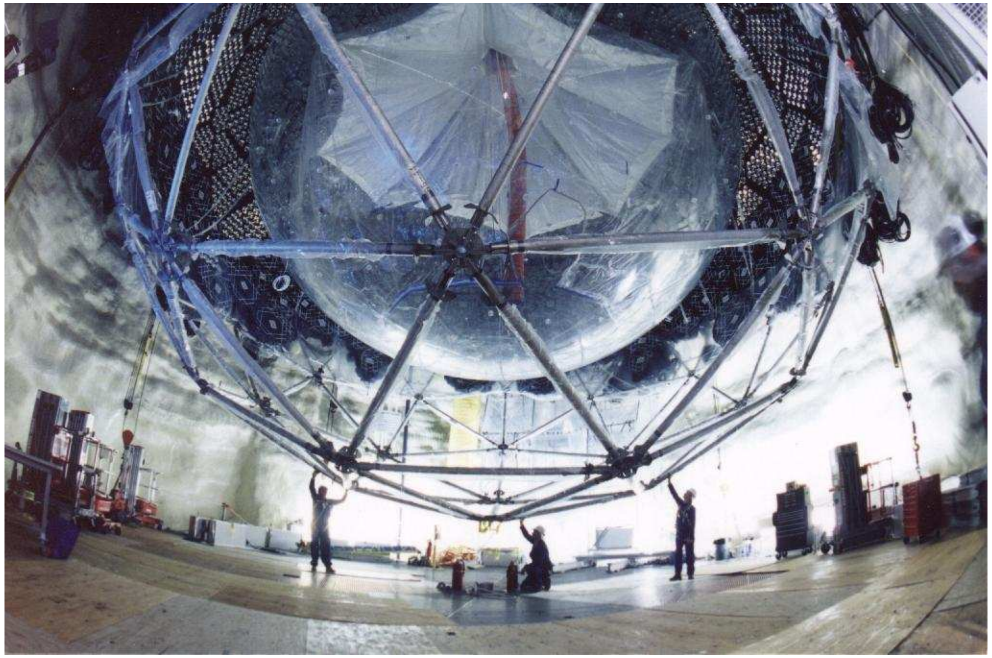

courtesy SNO

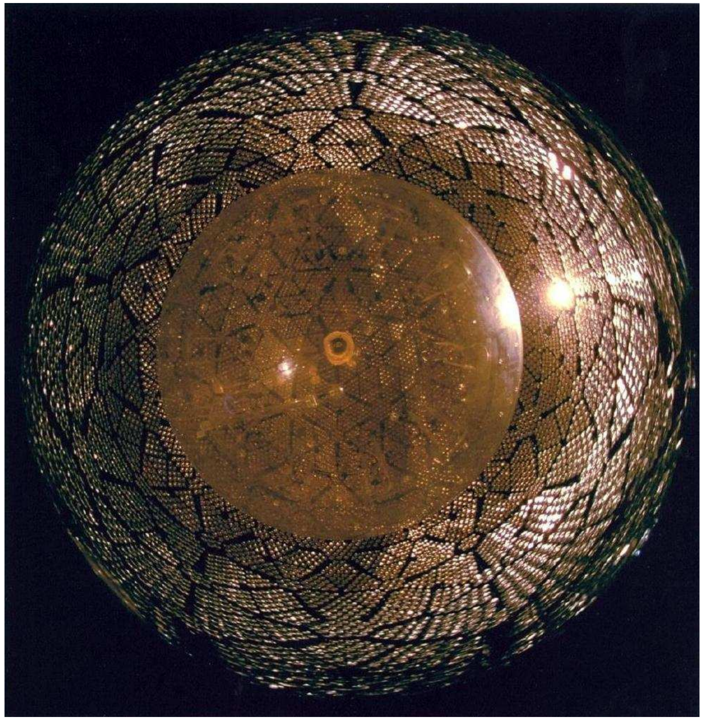

Acrylic vessel surrounded by photomultiplier tubes.

View through fisheye lens.

courtesy SNO

VOLUME 87, NUMBER 7 PHYSICAL REVIEW LETTERS 13 AUGUST 2001

Measurement of the Rate of $\nu_e + d \rightarrow p + p + e^-$ Interactions Produced by ^{8}B Solar Neutrinos at the Sudbury Neutrino Observatory

Q. R. Ahmad,[15] R. C. Allen,[11] T. C. Andersen,[12] J. D. Anglin,[7] G. Bühler,[11] J. C. Barton,[13,*] E. W. Beier,[14] M. Bercovitch,[7] J. Bigu,[4] S. Biller,[13] R. A. Black,[13] I. Blevis,[3] R. J. Boardman,[13] J. Boger,[2] E. Bonvin,[9] M. G. Boulay,[9] M. G. Bowler,[13] T. J. Bowles,[6] S. J. Brice,[6,13] M. C. Browne,[15] T. V. Bullard,[15] T. H. Burritt,[15,6] K. Cameron,[12] J. Cameron,[13] Y. D. Chan,[5] M. Chen,[9] H. H. Chen,[11,†] X. Chen,[5,13] M. C. Chon,[12] B. T. Cleveland,[13] E. T. H. Clifford,[9,1] J. H. M. Cowan,[4] D. F. Cowen,[14] G. A. Cox,[15] Y. Dai,[9] X. Dai,[13] F. Dalnoki-Veress,[3] W. F. Davidson,[7] P. J. Doe,[15,11,6] G. Doucas,[13] M. R. Dragowsky,[6,5] C. A. Duba,[15] F. A. Duncan,[9] J. Dunmore,[13] E. D. Earle,[9,1] S. R. Elliott,[15,6] H. C. Evans,[9] G. T. Ewan,[9] J. Farine,[3] H. Fergani,[13] A. P. Ferraris,[13] R. J. Ford,[9] M. M. Fowler,[6] K. Frame,[13] E. D. Frank,[14] W. Frati,[14] J. V. Germani,[15,6] S. Gil,[10] A. Goldschmidt,[6] D. R. Grant,[3] R. L. Hahn,[2] A. L. Hallin,[9] E. D. Hallman,[4] A. Hamer,[6,9] A. A. Hamian,[15] R. U. Haq,[4] C. K. Hargrove,[3] P. J. Harvey,[9] R. Hazama,[15] R. Heaton,[9] K. M. Heeger,[15] W. J. Heintzelman,[14] J. Heise,[10] R. L. Helmer,[10,‡] J. D. Hepburn,[9,1] H. Heron,[13] J. Hewett,[4] A. Hime,[6] M. Howe,[15] J. G. Hykawy,[4] M. C. P. Isaac,[5] P. Jagam,[12] N. A. Jelley,[13] C. Jillings,[9] G. Jonkmans,[4,1] J. Karn,[12] P. T. Keener,[14] K. Kirch,[6] J. R. Klein,[14] A. B. Knox,[13] R. J. Komar,[10,9] R. Kouzes,[8] T. Kutter,[10] C. C. M. Kyba,[14] J. Law,[12] I. T. Lawson,[12] M. Lay,[13] H. W. Lee,[9] K. T. Lesko,[5] J. R. Leslie,[9] I. Levine,[3] W. Locke,[13] M. M. Lowry,[8] S. Luoma,[4] J. Lyon,[13] S. Majerus,[13] H. B. Mak,[9] A. D. Marino,[5] N. McCauley,[13] A. B. McDonald,[9,8] D. S. McDonald,[14] K. McFarlane,[3] G. McGregor,[13] W. McLatchie,[9] R. Meijer Drees,[15] H. Mes,[3] C. Mifflin,[3] G. G. Miller,[6] G. Milton,[1] B. A. Moffat,[9] M. Moorhead,[13,5] C. W. Nally,[10] M. S. Neubauer,[14] F. M. Newcomer,[14] H. S. Ng,[10] A. J. Noble,[3,‡] E. B. Norman,[5] V. M. Novikov,[3] M. O'Neill,[3] C. E. Okada,[5] R. W. Ollerhead,[12] M. Omori,[13] J. L. Orrell,[15] S. M. Oser,[14] A. W. P. Poon,[5,6,10,15] T. J. Radcliffe,[9] A. Roberge,[4] B. C. Robertson,[9] R. G. H. Robertson,[15,6] J. K. Rowley,[2] V. L. Rusu,[14] E. Saettler,[4] K. K. Schaffer,[15] A. Schuelke,[5] M. H. Schwendener,[4] H. Seifert,[4,6,15] M. Shatkay,[3] J. J. Simpson,[12] D. Sinclair,[3] P. Skensved,[9] A. R. Smith,[5] M. W. E. Smith,[15] N. Starinsky,[3] T. D. Steiger,[15] R. G. Stokstad,[5] R. S. Storey,[7,†] B. Sur,[1,9] R. Tafirout,[4] N. Tagg,[12] N. W. Tanner,[13] R. K. Taplin,[13] M. Thorman,[13] P. Thornewell,[6,13,15] P. T. Trent,[13,*] Y. I. Tserkovnyak,[10] R. Van Berg,[14] R. G. Van de Water,[14,6] C. J. Virtue,[4] C. E. Waltham,[10] J.-X. Wang,[12] D. L. Wark,[13,6,§] N. West,[13] J. B. Wilhelmy,[6] J. F. Wilkerson,[15,6] J. Wilson,[13] P. Wittich,[14] J. M. Wouters,[6] and M. Yeh[2]

(SNO Collaboration)

[1] *Atomic Energy of Canada Limited, Chalk River Laboratories, Chalk River, Ontario K0J 1J0 Canada*
[2] *Chemistry Department, Brookhaven National Laboratory, Upton, New York 11973-5000*
[3] *Carleton University, Ottawa, Ontario K1S 5B6 Canada*
[4] *Department of Physics and Astronomy, Laurentian University, Sudbury, Ontario P3E 2C6 Canada*
[5] *Institute for Nuclear and Particle Astrophysics and Nuclear Science Division, Lawrence Berkeley National Laboratory, Berkeley, California 94720*
[6] *Los Alamos National Laboratory, Los Alamos, New Mexico 87545*
[7] *National Research Council of Canada, Ottawa, Ontario K1A 0R6 Canada*
[8] *Department of Physics, Princeton University, Princeton, New Jersey 08544*
[9] *Department of Physics, Queen's University, Kingston, Ontario K7L 3N6 Canada*
[10] *Department of Physics and Astronomy, University of British Columbia, Vancouver, BC V6T 1Z1 Canada*
[11] *Department of Physics, University of California, Irvine, California 92717*
[12] *Physics Department, University of Guelph, Guelph, Ontario N1G 2W1 Canada*
[13] *Nuclear and Astrophysics Laboratory, University of Oxford, Keble Road, Oxford, OX1 3RH, United Kingdom*
[14] *Department of Physics and Astronomy, University of Pennsylvania, Philadelphia, Pennsylvania 19104-6396*
[15] *Center for Experimental Nuclear Physics and Astrophysics, and Department of Physics, University of Washington, Seattle, Washington 98195*

(Received 18 June 2001; published 25 July 2001)

Solar neutrinos from ^{8}B decay have been detected at the Sudbury Neutrino Observatory via the charged current (CC) reaction on deuterium and the elastic scattering (ES) of electrons. The flux of ν_e's is measured by the CC reaction rate to be $\phi^{\text{CC}}(\nu_e) = 1.75 \pm 0.07(\text{stat})^{+0.12}_{-0.11}(\text{syst}) \pm 0.05(\text{theor}) \times 10^6\ \text{cm}^{-2}\,\text{s}^{-1}$. Comparison of $\phi^{\text{CC}}(\nu_e)$ to the Super-Kamiokande Collaboration's precision value of the flux inferred from the ES reaction yields a 3.3σ difference, assuming the systematic uncertainties are normally distributed, providing evidence of an active non-ν_e component in the solar flux. The total flux of active ^{8}B neutrinos is determined to be $5.44 \pm 0.99 \times 10^6\ \text{cm}^{-2}\,\text{s}^{-1}$.

DOI: 10.1103/PhysRevLett.87.071301 PACS numbers: 26.65.+t, 14.60.Pq, 95.85.Ry

071301-1 0031-9007/01/87(7)/071301(6)$15.00 © 2001 The American Physical Society 071301-1

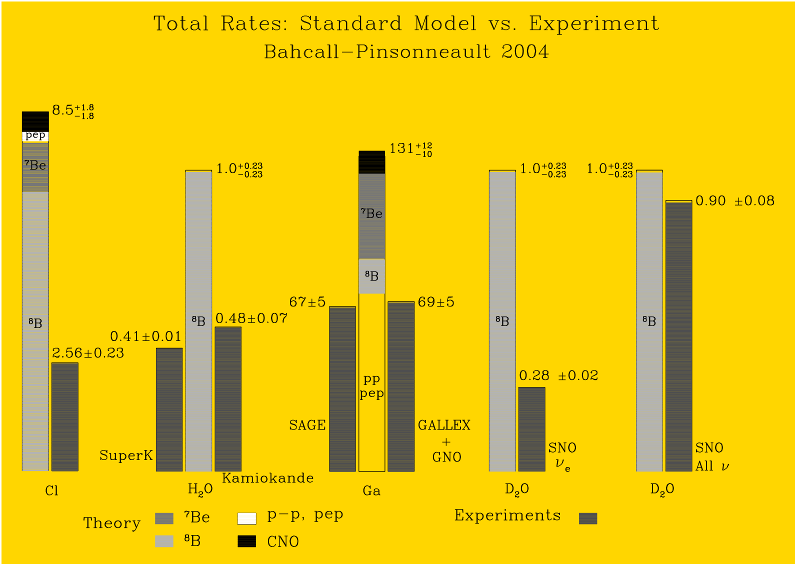

Bahcall

SNO (2001): When taking *all* neutrino flavors into account, the measured and predicted neutrino fluxes agree ⟹ Neutrinos change their flavor.

Solar Neutrinos

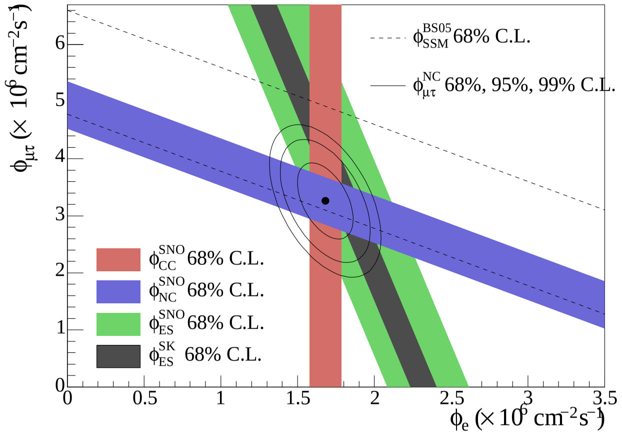

Aharmin et al., 2005 (dashed line: prediction of standard solar model)

SNO (2001): 2/3 of all ν_e produced in Sun change into ν_τ or ν_μ on their way from Sun to Earth: neutrino oscillations ⟹ physics beyond the standard model of particle physics!

Main Sequence

Main Sequence in the Hertzsprung-Russell-Diagram:

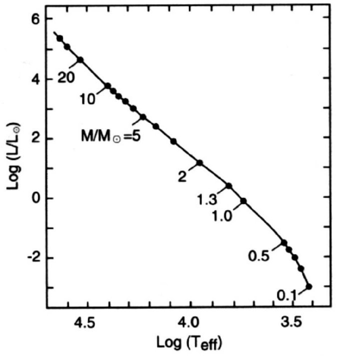

Masses along the HRD

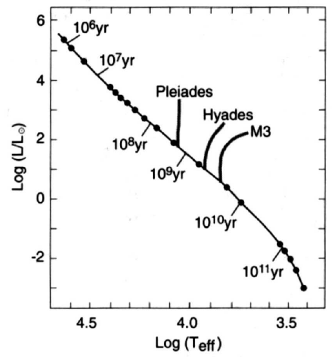

life times along the HRD

mass limits: Min.: 0.08$M_\odot$ (no H-burning for lower masses)

Max.: $\approx$ 100 $M_\odot$ (radiation pressure too high, $p_{\rm rad} \sim T_{\rm eff}^4$)

Main Sequence

Properties of Main Sequence stars:

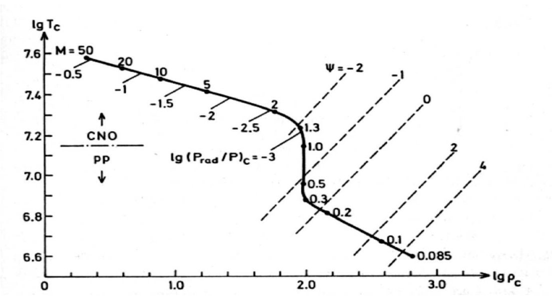

Central temperatures & densities

- strong change at $\approx 1M_\odot$
- low masses ($< 0.5M_\odot$): low temperature, very high density
- high masses ($> 1.3M_\odot$): high temperature, low density
- low mass stars burn H in the pp-chains
- high mass stars burn H in the CNO-cycle

Main Sequence

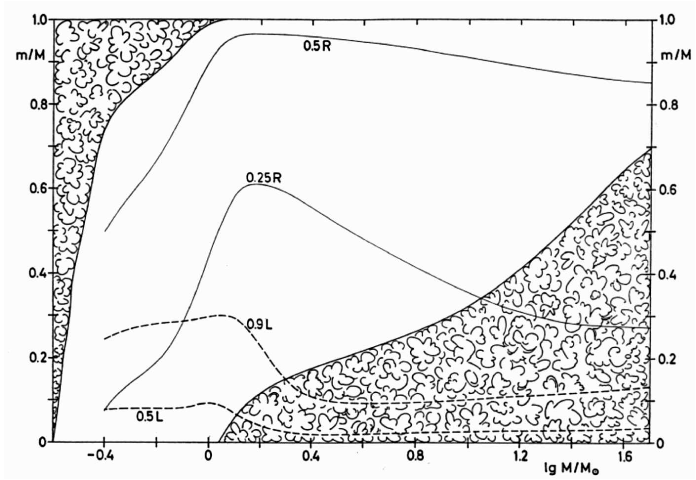

Kippenhahn-diagram: Internal Structure of Main Sequnece stars

---

Main Sequence

Empirical test of main sequence models:

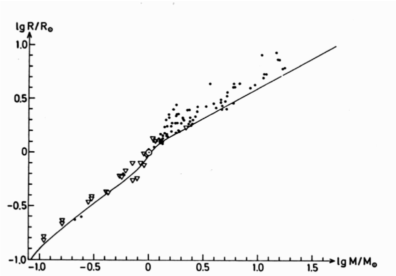

Mass–Radius relation

$R \sim M^a$

lower main sequence: $a \approx 0.8$
upper main sequence: $a \approx 0.6$

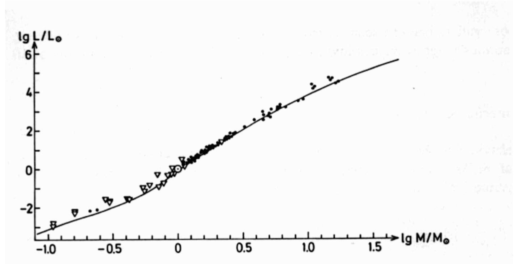

Mass–Luminosity relation

$L \sim M^b$

$b = 2.3$ for $M < 0.43\,M_\odot$
$b = 4.0$ for $M > 0.43\,M_\odot$

Main Sequence Evolution

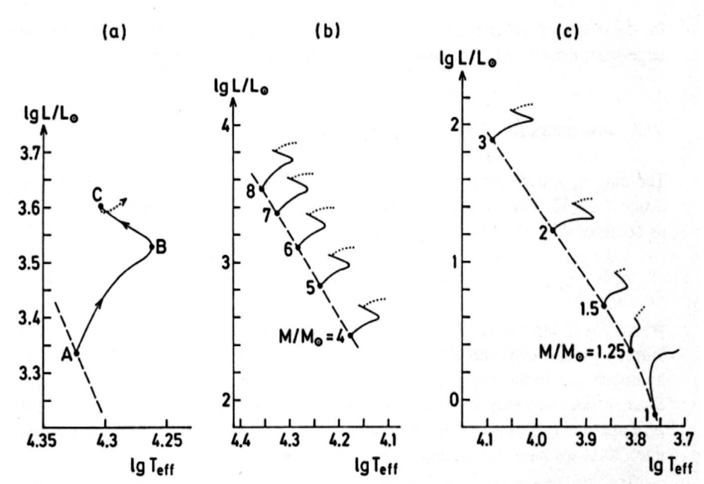

main sequence evolution from zero age to helium exhaustion

Post Main Sequence

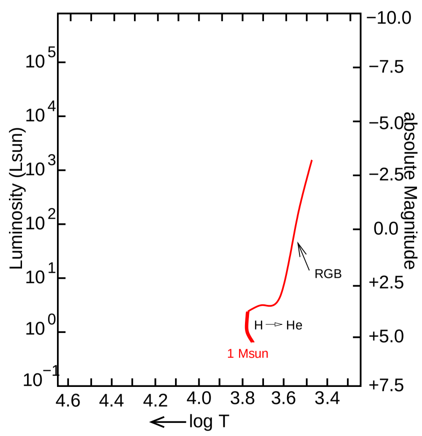

(after Iben, 1991)

Once H is exhausted in center: H continues to burn in a shell around the He core ("shell burning").

For stars with $M \lesssim 1\,M_\odot$: Star reacts by expanding convective envelope until it is almost fully convective.

$\Longrightarrow$ luminosity increases, temperature decreases

$\Longrightarrow$ motion in HRD horizontally towards the right, then upwards to higher L: red giant stage.

Post Main Sequence

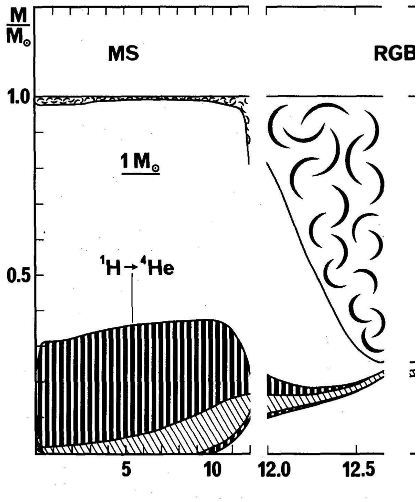

(Maeder & Meynet, 1989)

Once H is exhausted in center: H continues to burn in a shell around the He core ("shell burning").

For stars with $M \lesssim 1\,M_\odot$: Star reacts by expanding convective envelope until it is almost fully convective.

Post Main Sequence

Reminder: stars are in hydrostatic equilibrium: inwards gravitational pressure balanced by outwards gas pressure

Since the gas pressure is $P = nkT$: energy source needed to heat gas (=fusion).

This is a problem for the core during the red giant stage, as virtually no fusion ongoing

$\Longrightarrow$ Core gets compressed

$\Longrightarrow$ ρ and T increase

BUT:

collapse cannot continue indefinitely!

$\Longrightarrow$ once ρ has increased appreciably, there must be a point where quantum mechanical effects become important.

QM interlude

Quantum mechanics: The Pauli exclusion principle:

For particles such as electrons (“Fermions”), at least one of their quantum numbers must be different.

Quantum numbers are, e.g.,

- position (x, y, z),
- momentum p ($p_x = mv_x$, $p_y = mv_y$, $p_z = mv_z$),
- angular momentum,
- spin (s)

All of these numbers are “quantized”, i.e., can only have discrete values (e.g., spin: $+1/2$, $-1/2$).

Heisenberg’s principle: (6-d) phase space is quantized: $\Delta p \times \Delta V \approx h^3$

Each cell in phase space can host two electrons of different spin

In a typical gas, this is not a problem (“phase space is (almost) empty”) once it becomes dense $\Longrightarrow$ exclusion principle kicks in.

QM interlude

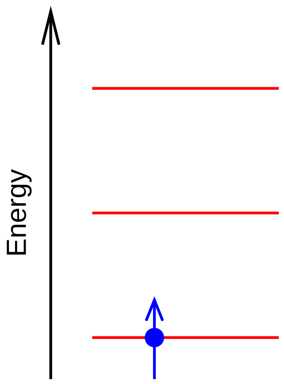

Effect of high density on electron energy

Energy of electrons at the same position in space

QM interlude

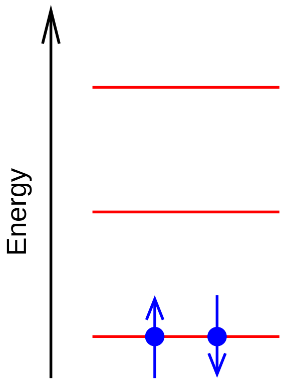

Effect of high density on electron energy

Energy of electrons at the same position in space

QM interlude

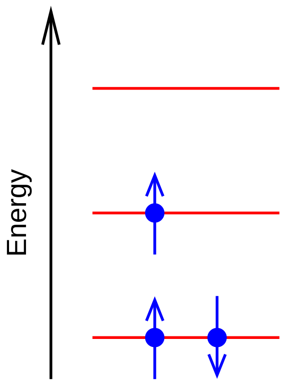

Effect of high density on electron energy

Energy of electrons at the same position in space

QM interlude

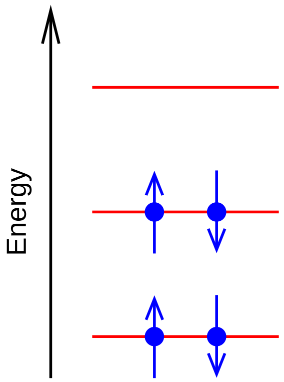

Energy of electrons at the same position in space

Effect of high density on electron energy

QM interlude

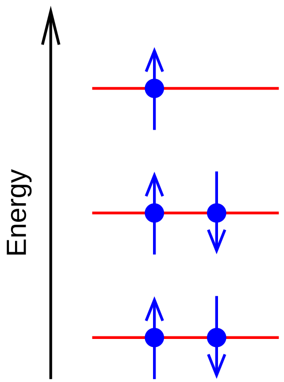

Energy of electrons at the same position in space

Effect of high density on electron energy

QM interlude

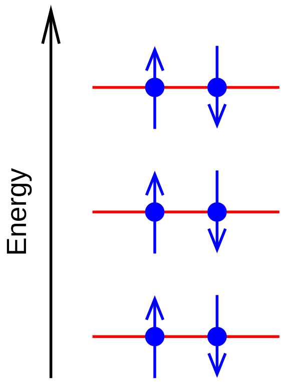

Energy of electrons at the same position in space

Effect of high density on electron energy:

In degenerate electron gases, electrons have much higher energies than in thermal gas.

QM interlude

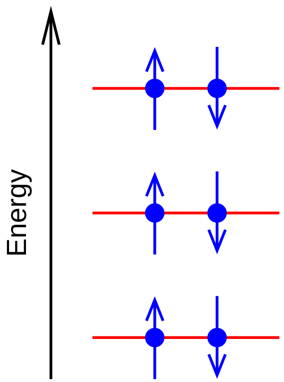

Energy of electrons at the same position in space

Effect of high density on electron energy:

In degenerate electron gases, electrons have much higher energies than in thermal gas.

Interaction of electrons results in degeneracy pressure:

$$P = \frac{\hbar^2}{m_\mathrm{e}} n_\mathrm{e}^{5/3} \propto \rho^{5/3}$$

Note: The degeneracy pressure is independent of the temperature!

Post Main Sequence

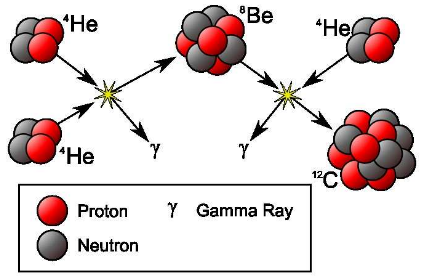

In the degenerate core, once $T_{\rm core} \sim 100 \times 10^6$ K: Triple alpha process starts:

$$^4\text{He} + {}^4\text{He} \leftrightarrow {}^8\text{Be}$$
$$^8\text{Be} + {}^4\text{He} \rightarrow {}^{12}\text{C}$$

Since ^{8}Be has a half life of only 2.6×10^{-16} s: this can only work effectively if 3 α-particles collide.

But core is degenerate:

$\Longrightarrow$ High thermal conductivity of electrons
$\Longrightarrow$ core has uniform temperature
$\Longrightarrow$ 3α onset is rapid
$\Longrightarrow$ He flash

Not seen on surface (“buffered” by convective envelope).

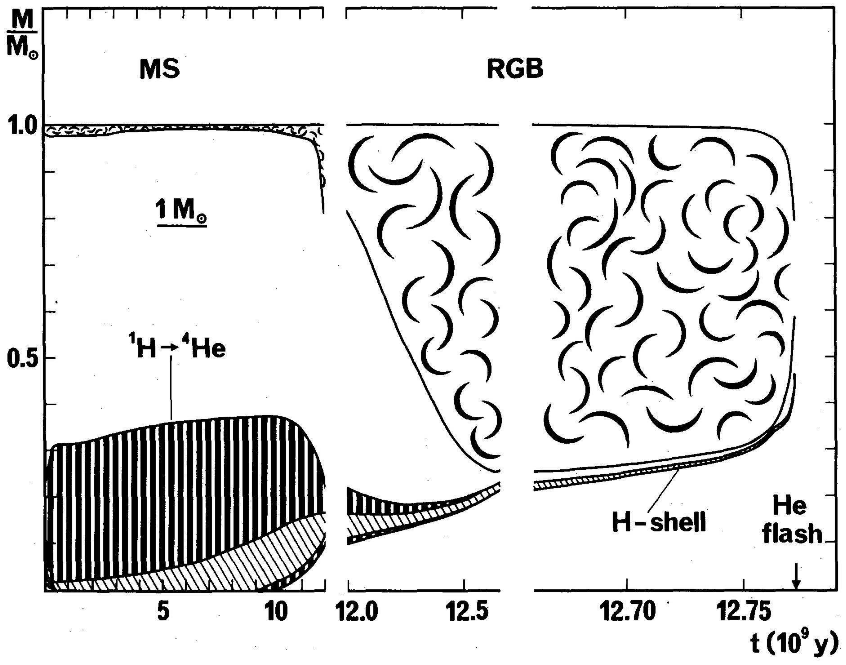

Evolution of the structure of a 1 $M_\odot$ star to the Helium flash (Maeder & Meynet, 1989).

Post Main Sequence

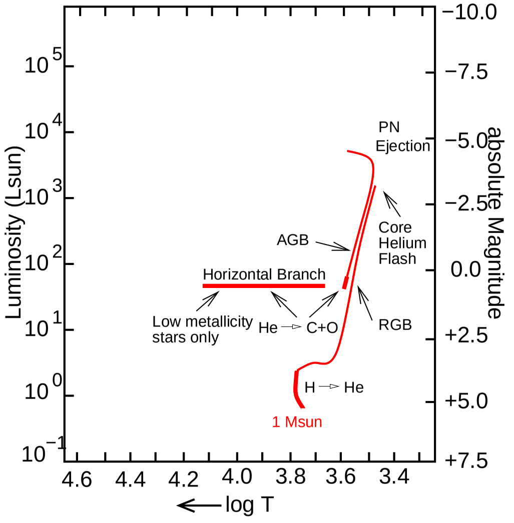

After the He flash star has He burning in core and H shell burning

$\Longrightarrow$ starts to expand again

$\Longrightarrow$ “asymptotic giant branch”

Instable He fusion processes (“thermal pulses”) lead to ejection of outer layers (∼50% of total mass!)

Effect of He core being unable to transport energy away quickly enough.

$\Longrightarrow$ inner (hotter) parts of star become visible.

after Iben, 1991

Abell 39 (WIYN, AURA, NOAO, NSF)

planetary nebulae: material ejected during AGB phase, photoionized once remaining core of former star has shed enough mass to emit UV photons.

Ring Nebula (HST/STScI/NASA)

planetary nebulae: material ejected during AGB phase, photoionized once remaining core of former star has shed enough mass to emit UV photons.

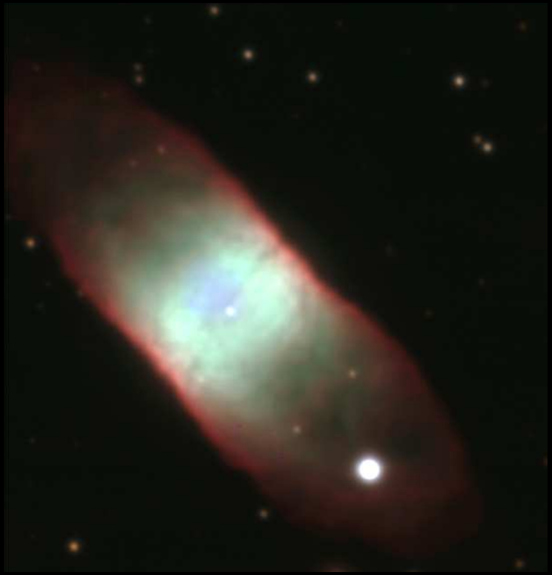

IC4406 (ESO VLT)

planetary nebulae: material ejected during AGB phase, photoionized once remaining core of former star has shed enough mass to emit UV photons.

NGC 6853/M27 (“Dumbbell Nebula”; ESO VLT/FORS)

planetary nebulae: material ejected during AGB phase, photoionized once remaining core of former star has shed enough mass to emit UV photons.

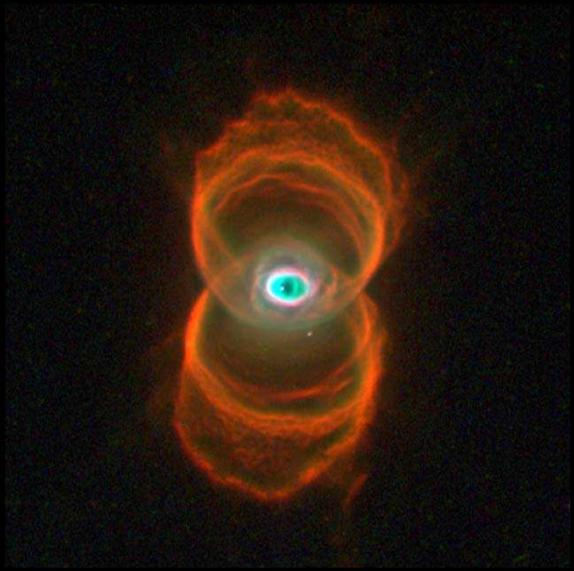

Hourglass Nebula (HST/Sahai/Trauger)

planetary nebulae: material ejected during AGB phase, photoionized once remaining core of former star has shed enough mass to emit UV photons.

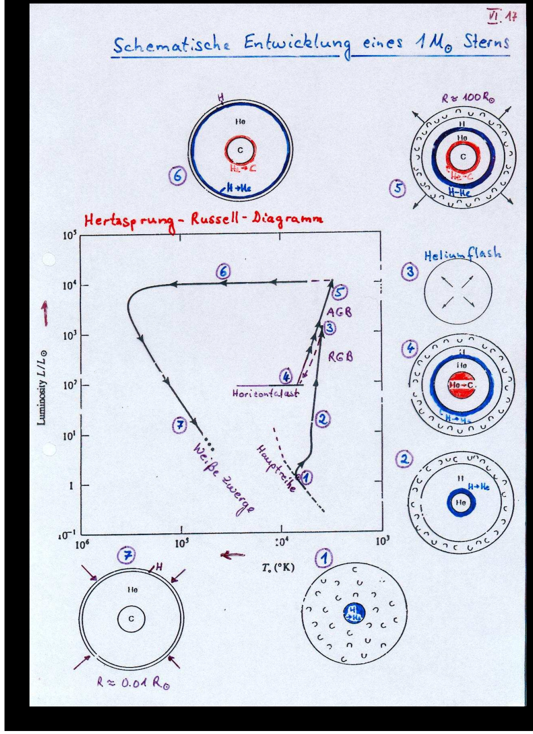

Summary: Evolution of Low Mass Stars:

1. =
2.
   =
3.
   = helium ignition in degenerate electron gas
4.
   =
5.
   = Tip of AGB: envelope ejection through dust formation & pulsations
6. hot star excites the ejected envelope to shine
7. =

Stars born with masses $> 8\,M_\odot$

Evolution on MS similar, however, faster than for low mass stars.

More massive stars reach threshold temperature for 3α and subsequent nuclear burning before reaching degeneracy

$\Longrightarrow$ He just starts to burn.

In these objects, higher order fusion processes can kick in (but are energetically unimportant): alpha reactions

$$\begin{aligned} {}^{12}\mathrm{C} + {}^{4}\mathrm{He} &\rightarrow {}^{16}\mathrm{O} + \gamma \\ {}^{16}\mathrm{O} + {}^{4}\mathrm{He} &\rightarrow {}^{20}\mathrm{Ne} + \gamma \\ {}^{20}\mathrm{Ne} + {}^{4}\mathrm{He} &\rightarrow {}^{24}\mathrm{Mg} + \gamma \end{aligned}$$

Outer layers continue H shell burning.

During evolution of star on red giant branch: convective envelope moves deeper into core, can mix fusion products into outer layers.

Reminder: Main Sequence

Structure on the Main Sequence: Simulations show existence of two regimes:

lower main sequence : stars have structure similar to Sun:

- energy generation: pp-chain ($\epsilon \propto T^5$)
- inner radiative core
- convective envelope

upper main sequence : for central temperatures of 18 $\times$ 10^6 K (1.5 $M_\odot$ stars): pp-chain and CNO-cycle produce equal amounts of energy. Above that: CNO dominates.

- energy generation: CNO-cycle ($\epsilon \propto T^{17}$)
- inner convective core since energy generation from CNO cycle strongly peaked towards center.
- outer radiative envelope

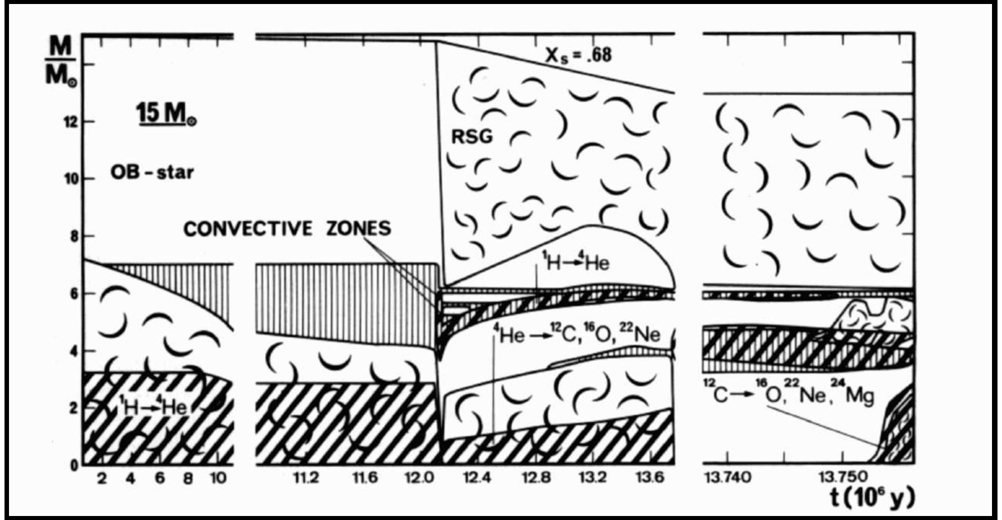

Evolution of the star.

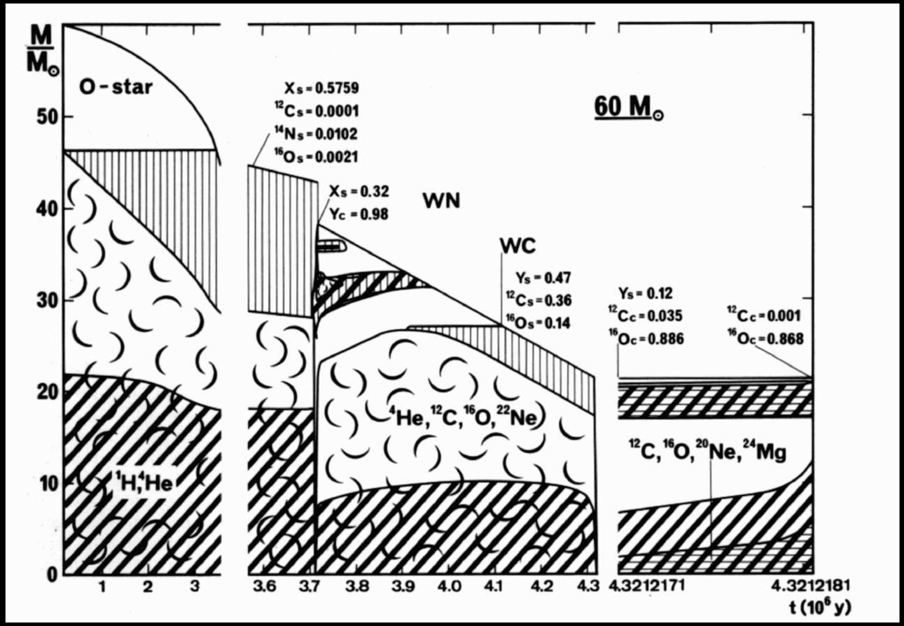

Evolution of the star.

Note the very strong mass loss!

Stars born with masses $> 8\,M_\odot$

Nuclear reactions in massive ($> 8\,M_\odot$) stars:

Reaction	above T [10^6 K]	Energy gain [MeV]
Hydrogen burning		
$4\,^1\mathrm{H} \longrightarrow {}^4\mathrm{He}$	4	6.55
Helium burning		
$3\,^4\mathrm{He} \longrightarrow {}^8\mathrm{Be} + {}^4\mathrm{He} \longrightarrow {}^{12}\mathrm{C}$	100	<0.61
Carbon burning		
$^{12}\mathrm{C} + {}^4\mathrm{He} \longrightarrow {}^{16}\mathrm{O}$	600	<0.54
$2\,^{12}\mathrm{C} \longrightarrow {}^4\mathrm{He} + {}^{20}\mathrm{Ne}$		
$^{20}\mathrm{Ne} + {}^4\,\mathrm{He} \longrightarrow \mathrm{n} + {}^{23}\mathrm{Mg}$		
Oxygen burning		
$2\,^{16}\mathrm{O} \longrightarrow {}^4\mathrm{He} + {}^{28}\mathrm{Si}$	1000	<0.3
$2\,^{16}\mathrm{O} \longrightarrow 2\,^4\mathrm{He} + {}^{24}\mathrm{Mg}$		
Silicon burning		
$2\,^{28}\mathrm{Si} \longrightarrow {}^{56}\mathrm{Fe}$	3000	< 0.18

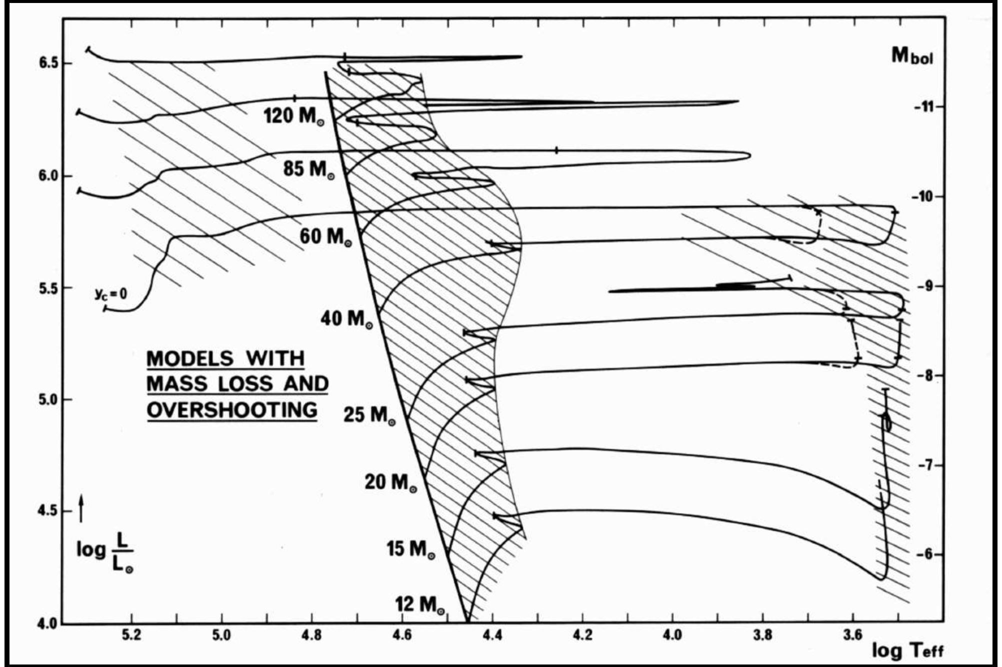

Summary: Evolution of in the HRD.

Stars born with masses $> 8\,M_\odot$

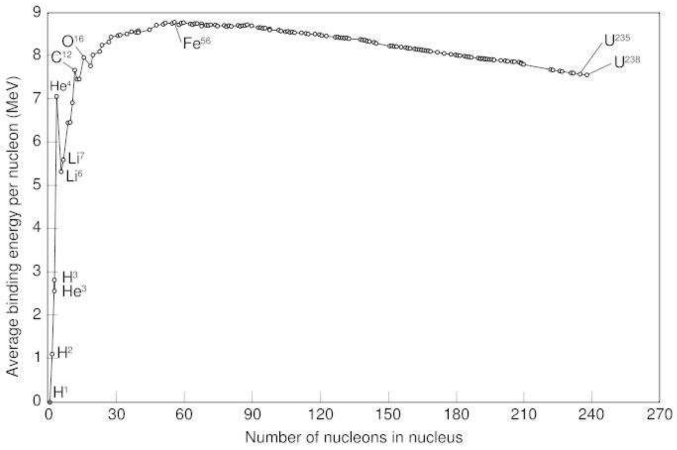

^{56}Fe is one of the most tightly bound nucleons ⟹ Star has a problem once ^{56}Fe reached: fusion processed become endotherm

Stars born with masses $> 8\,M_\odot$

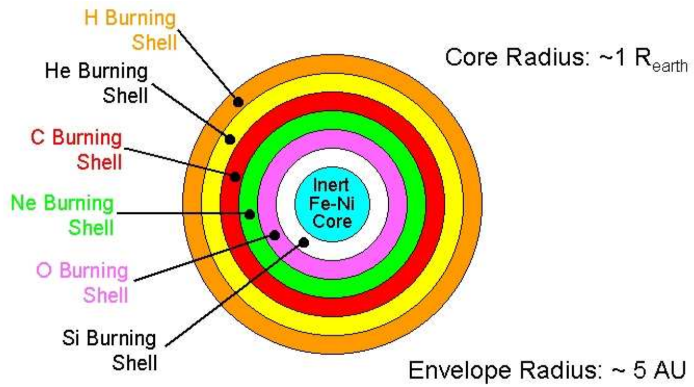

successive stages of nuclear burning: final state: onion-shell model

1. H burning, ash: He
2. He burning, ashes: C, O, Ne, Mg
3. C burning, ashes: Ne, Na, Mg
4. Ne burning, ashes: O, Mg . . .
5. O burning, ashes: Si, P, S, . . .
6. Si burning, ashes: Fe, Ni